

## HST SNAPSHOT STUDY OF VARIABLE STARS IN GLOBULAR CLUSTERS: INNER REGION OF NGC 6441<sup>1</sup>

BARTON J. PRITZL<sup>2,3</sup>, HORACE A. SMITH<sup>2</sup>, PETER B. STETSON<sup>4</sup>, MÁRCIO CATELAN<sup>5</sup>, ALLEN V.  
SWEIGART<sup>6</sup>, ANDREW C. LAYDEN<sup>7</sup>, R. MICHAEL RICH<sup>8</sup>  
*AJ, in press*

### ABSTRACT

We present the results of a *Hubble Space Telescope* snapshot program to survey the inner region of the metal-rich globular cluster NGC 6441 for its variable stars. A total of 57 variable stars was found including 38 RR Lyrae stars, 6 Population II Cepheids, and 12 long period variables. Twenty-four of the RR Lyrae stars and all of the Population II Cepheids were previously undiscovered in ground-based surveys. Of the RR Lyrae stars observed in this survey, 26 are pulsating in the fundamental mode with a mean period of 0.753 d and 12 are first-overtone mode pulsators with a mean period of 0.365 d. These values match up very well with those found in ground-based surveys. Combining all the available data for NGC 6441, we find mean periods of 0.759 d and 0.375 d for the RRab and RRc stars, respectively. We also find that the RR Lyrae in this survey are located in the same regions of a period-amplitude diagram as those found in ground-based surveys. The overall ratio of RRc to total RR Lyrae is 0.33. Although NGC 6441 is a metal-rich globular cluster and would, on that ground, be expected either to have few RR Lyrae stars, or to be an Oosterhoff type I system, its RR Lyrae more closely resemble those in Oosterhoff type II globular clusters. However, even compared to typical Oosterhoff type II systems, the mean period of its RRab stars is unusually long. We also derived *I*-band period-luminosity relations for the RR Lyrae stars.

Of the six Population II Cepheids, five are of W Virginis type and one is a BL Herculis variable star. This makes NGC 6441, along with NGC 6388, the most metal-rich globular cluster known to contain these types of variable stars. Another variable, V118, may also be a Population II Cepheid given its long period and its separation in magnitude from the RR Lyrae stars. We examine the period-luminosity relation for these Population II Cepheids and compare it to those in other globular clusters and in the Large Magellanic Cloud. We argue that there does not appear to be a change in the period-luminosity relation slope between the BL Herculis and W Virginis stars, but that a change of slope does occur when the RV Tauri stars are added to the period-luminosity relation.

*Subject headings:* Stars: variables: RR Lyrae stars; Galaxy: globular cluster: individual (NGC 6441)

### 1. INTRODUCTION

Globular clusters (GCs) are tracers of the formation of the galaxy to which they belong. One key way to analyze the stellar populations of a GC is to determine its RR Lyrae (RRL) content, which is tied to the horizontal branch (HB) morphology. Oosterhoff (1939) discovered a fundamental division of Galactic GCs into two groups based on the mean periods of their RRL stars. It was later shown that this division was associated with GC metallicity: Metal-rich GCs tend to have shorter period RRL stars compared to metal-poor GCs (Arp 1955b; Kinman 1959). Understanding the Oosterhoff effect and its effect on RRL stars is key for determining accurate distances and ages for the Galactic GCs, and ultimately has consequences on how we view the formation of our Galaxy.

Sandage & Wildey (1967) and van den Bergh (1967) found that a number of metal-poor GCs have very different HB morphologies even though they have very similar values of [Fe/H]. It was concluded that at least one parameter, in addition to

metallicity, affects the HB. They also pointed out that the most distant GCs exhibited strong second parameter effects, having red HBs despite their low metallicities. Since then it has been shown that a GC's galactocentric distance plays a role in the strength of the second parameter in the sense that at small galactocentric distances the HB morphology and [Fe/H] are closely tied to one another, while going out to larger distances one finds that there is more scatter in the HB morphologies, with the HB type becoming redder for a given [Fe/H] (Searle & Zinn 1978; Zinn 1980; Lee, Demarque, & Zinn 1994). A difference in cluster ages has been proposed as one explanation for the second parameter effect, but there are cases where this may not be the only explanation for unusual HB morphologies (e.g., Fusi Pecci, Bellazzini, & Ferraro 1996; Fusi Pecci & Bellazzini 1997). Any second-parameter affecting the HB morphology will also affect any RRL stars found in that cluster. Thus, as pointed out by Catelan, Sweigart, & Borissova (1998), RRL stars may also provide a probe into the second-parameter phenomenon, which in turn may be directly related to the origin of

<sup>1</sup> Based on observations with the NASA/ESA *Hubble Space Telescope*, obtained at the Space Telescope Science Institute, which is operated by the Association of Universities for Research in Astronomy, Inc., (AURA), under NASA Contract NAS 5-26555.

<sup>2</sup> Dept. of Physics and Astronomy, Michigan State University, East Lansing, MI 48824; pritzl@pa.msu.edu, smith@pa.msu.edu

<sup>3</sup> Current address: National Optical Astronomy Observatories, P.O. Box 26732, Tucson, AZ 85726; pritzl@noao.edu

<sup>4</sup> Dominion Astrophysical Observatory, Herzberg Institute of Astrophysics, National Research Council, 5071 West Saanich Road, Victoria, BC V9E 2E7, Canada; Peter.Stetson@nrc.gc.ca

<sup>5</sup> Pontificia Universidad Católica de Chile, Departamento de Astronomía y Astrofísica, Av. Vicuña Mackenna 4860, 782-0436 Macul, Santiago, Chile; mcate-lan@astro.puc.cl

<sup>6</sup> NASA Goddard Space Flight Center, Laboratory for Astronomy and Solar Physics, Code 681, Greenbelt, MD 20771; sweigart@bach.gsfc.nasa.gov

<sup>7</sup> Department of Physics and Astronomy, 104 Overman Hall, Bowling Green State University, Bowling Green, OH 43403; layden@baade.bgsu.edu

<sup>8</sup> Department of Physics and Astronomy, UCLA, 8979 Math-Sciences Building, Los Angeles, CA 90095-1562; rmn@astro.ucla.edu

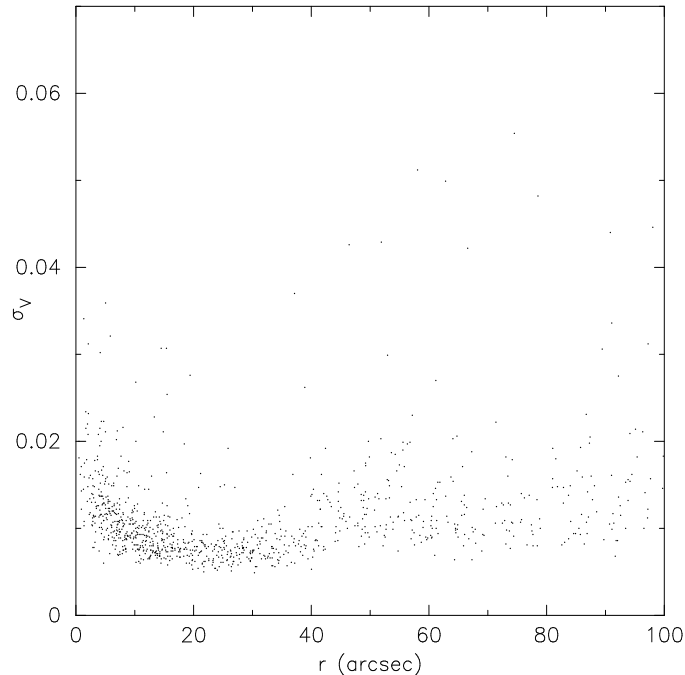


FIG. 1.— Photometric uncertainty as a function of clustercentric radius for stars at the horizontal branch level in NGC 6441. The consistency of the photometric uncertainty with radius proves that our errors are not due to crowding, but photon statistics and fitting errors.

the Oosterhoff dichotomy itself (Castellani 1983; Renzini 1983; Lee & Zinn 1990).

While the second-parameter effect has primarily been found in more metal-poor GCs, two metal-rich systems, NGC 6388 and NGC 6441, have been found to have very unusual HB morphologies for their metallicities (Rich et al. 1997). With metallicities of  $[\text{Fe}/\text{H}] \sim -0.6$  these clusters not only have strong red HBs similar to the canonical metal-rich GC 47 Tucanae, they also have components to their HBs that extend blueward across the instability strip and terminate in blue tails. In addition, the red HBs in both clusters are sloped toward increasing brightness as one moves blueward along the HB, which cannot be explained by differential reddening alone. To make these GCs even more interesting, Sweigart & Catelan (1998) have claimed that non-canonical effects are needed to explain the sloped nature of the HBs. Rich et al. speculated that the high central concentrations of NGC 6388 and NGC 6441 may have led to higher interactions in the inner regions of the clusters, resulting in the bluer HBs—without however providing an explanation for the sloping nature of the HBs. However, both Rich et al. and Layden et al. (1999) found that this hypothesis did not hold because the blue HB stars were not centrally concentrated.

In attempting to model the HBs in NGC 6388 and NGC 6441, Sweigart & Catelan (1998) proposed three alternatives, (i) a high cluster helium abundance, (ii) an increase in helium core mass due to rotation on the red giant branch, and (iii) enhancement of the envelope helium abundance due to deep mixing. The high helium abundance scenario has subsequently been ruled out on observational grounds (Layden et al. 1999; Raimondo et al. 2002). Other explanations for these unusual HB morphologies have ranged from increased mass loss along the red giant branch, to a spread in metallicity, to the clusters being dwarf galaxy remnants (Piotto et al. 1997; Sweigart 2002; Ree et al. 2002).

All three scenarios introduced by Sweigart & Catelan (1998) require that the HBs of NGC 6388 and NGC 6441 be unusually

bright for the metal abundances of the clusters. As a consequence, any RRL stars found in these clusters would also be unusually bright and would therefore have unusually long periods for their metallicity. Surveys of the variable star content of NGC 6388 (Silbermann et al. 1994; Pritzl et al. 2002) and NGC 6441 (Layden et al. 1999; Pritzl et al. 2001) found that their RRL stars did indeed have periods that are unusually long for the cluster metallicity. On the other hand, the gravities (for the hot HB stars) measured by Moehler, Sweigart, & Catelan (1999) imply that the blue HB stars in these clusters are not anomalously bright, contrary to the Sweigart & Catelan (1998) predictions.

Due to the compact nature of these clusters [ $\log \rho (L_{\odot} \text{ pc}^{-3}) = 5.34$  (NGC 6388), 5.25 (NGC 6441)], it is very difficult to survey the inner regions of the clusters, where most of the cluster variables are expected to be found, from the ground. Making use of the *Hubble Space Telescope* (HST) snapshot program, we have obtained images of the inner region of NGC 6441 to survey its variable star content with the Wide Field Planetary Camera 2 (WFPC2). We present in this paper the results of our survey and compare the properties of the variable stars found in the inner region of the cluster to those variables found in the outer regions from the ground-based surveys. We also examine the nature of the Population II Cepheids (P2Cs) found in NGC 6441 and NGC 6388 and compare them with those in other GCs.

## 2. OBSERVATIONS AND REDUCTIONS

Eighteen sets of observations in *B*, *V*, and *I* were taken by the HST with the Wide-Field Planetary Camera 2 starting on 1999 March 16 and ending on 2000 June 30 as part of the SNAP 8251 program. The complete list of observations is given in Table 1, including NGC 6441 HST archive observations which were added to our reductions (GO 5667, GO 6095, and GO 6780). Exposure times for each filter are also listed in Table 1. NGC 6441 was centered on the WFC3 chip for

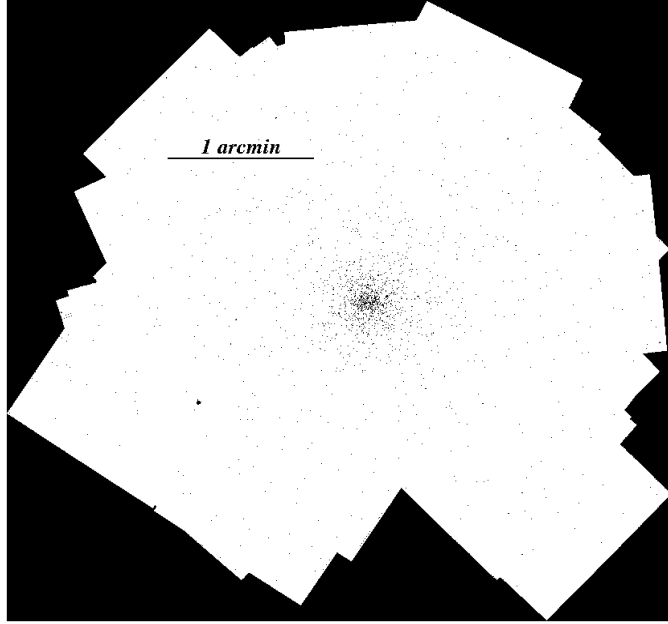


FIG. 2A.— NGC 6441 finding charts marking all of the variable stars found in this paper. Figure 2a shows the full field-of-view for our observations. The image is 283-by-267 arcseconds at maximum extent, with a scale of 22 pixels per arcsecond. North is up and east is to the left.

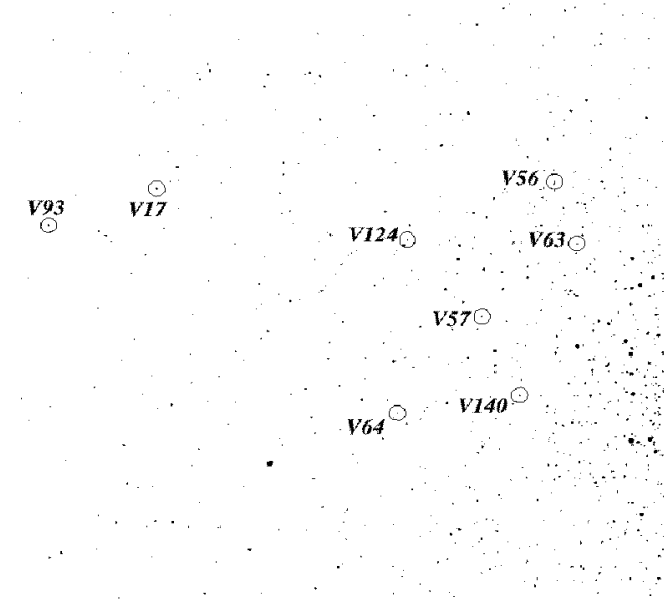


FIG. 2B.— NGC 6441 finding charts marking all of the variable stars found in this paper. Figure 2a shows the full field-of-view for our observations. The image is 283-by-267 arcseconds at maximum extent, with a scale of 22 pixels per arcsecond. North is up and east is to the left.

our program. No restrictions were made on the orientation of the observations. Therefore, rotations between the images, in addition to translations, produced partial and varying overlap among the images obtained on the other three chips.

The observations were reduced using the DAOPHOT/ ALLSTAR/ ALLFRAME routines (e.g., Stetson 1987, 1994). We used standard point-spread functions that had been prepared for each chip and filter in the course of the *Hubble Space Telescope Key Project on the Extragalactic Distance Scale* (e.g., Freedman et al. 2001; Stetson et al. 1998) and our previous research on outer-halo globulars (e.g., Harris et al. 1997, Stetson et al. 1999). After the geometric relationships relating the various images to a common coordinate system and a master star list

for the field had been generated, ALLFRAME was used to obtain final stellar positions on the sky, and a magnitude measurement for each star at each epoch. Aperture corrections were determined from comparatively bright, isolated stars in each image to relate them to a well-defined, common instrumental zero-point. Charge-transfer efficiency corrections and fundamental photometric zero-points similar to those of Stetson (1998), but based on a much larger database, and the color corrections of Holtzman et al. (1995) were applied in the standard fashion.

Figure 1 shows the photometric uncertainty in  $V$  at the level of the HB as a function of clustercentric radius. We assumed  $m_{V,RR} = 17.54$  mag and chose a range of magnitudes around this value of  $\pm 0.25$  mag. All candidate variable stars were removed.

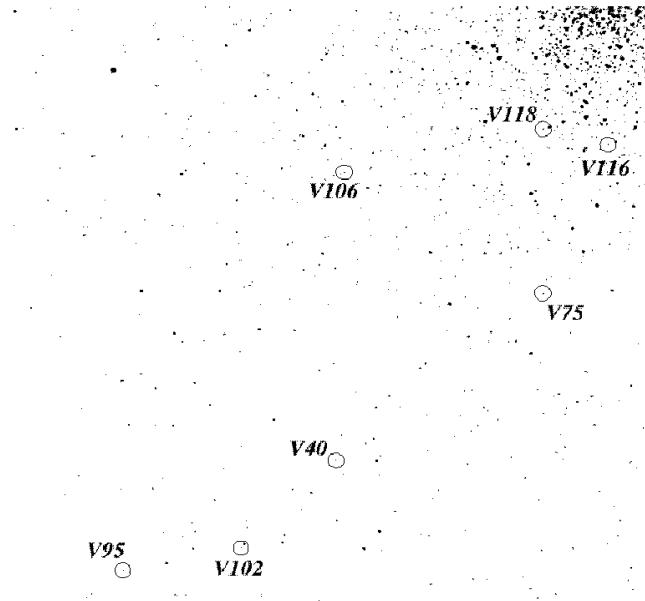


FIG. 2C.— NGC 6441 finding charts marking all of the variable stars found in this paper. Figure 2a shows the full field-of-view for our observations. The image is 283-by-267 arcseconds at maximum extent, with a scale of 22 pixels per arcsecond. North is up and east is to the left.

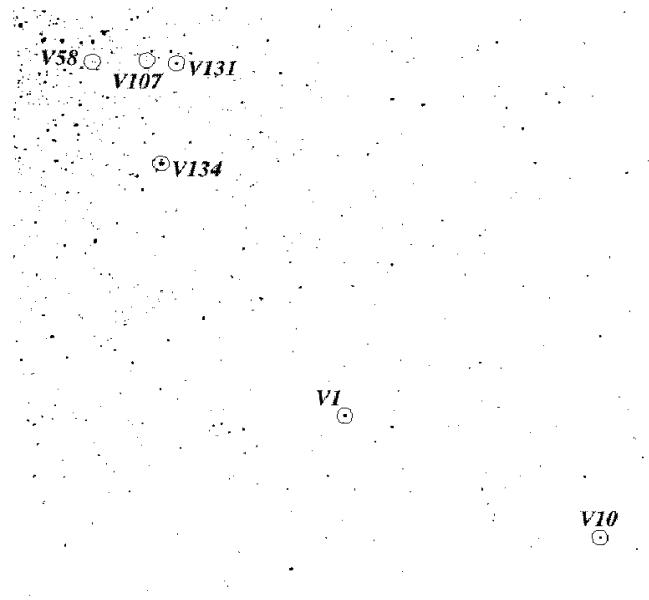


FIG. 2D.— NGC 6441 finding charts marking all of the variable stars found in this paper. Figure 2a shows the full field-of-view for our observations. The image is 283-by-267 arcseconds at maximum extent, with a scale of 22 pixels per arcsecond. North is up and east is to the left.

The  $\sigma_V$  relationship is nearly independent of radius. This suggests that at these limits our photometric errors are dominated by photon statistics and fitting errors and not by crowding for most stars. The increased photometric uncertainty at large radii occurs because, with the differing roll angles of the spacecraft, not all stars could be measured at all epochs.

Variable stars were found by a variety of methods including a variant of the Welch & Stetson (1993) algorithm (see Stetson 1996). Finding charts for the variables can be seen in Figure 2. We used the period finding routines described in Layden et al. (1999) and Layden & Sarajedini (2000) to determine the periods of the variable stars. This technique involves folding each star’s magnitude-time data by a sequence of periods, and at each

period, fitting the resulting light curve with a set of template light curves. If the period being tested is near the star’s true period, the template will fit the data well and produce a small value of  $\chi^2$ . Probable periods are represented by  $\chi^2$  minima in the array of periods and templates considered. We searched for periods in the range appropriate for each class of variable; e.g., for RRL stars the range was 0.2 to 1.0 day. Once a period was found, the search was narrowed to about 0.0001 day around the candidate period to determine the best period. In almost all cases, we found a single, dominant  $\chi^2$  minimum, suggesting that aliasing was not a problem despite the irregular sampling and long time interval over which the data were gathered. The few exceptions involved a small number of first-overtone (RRc)

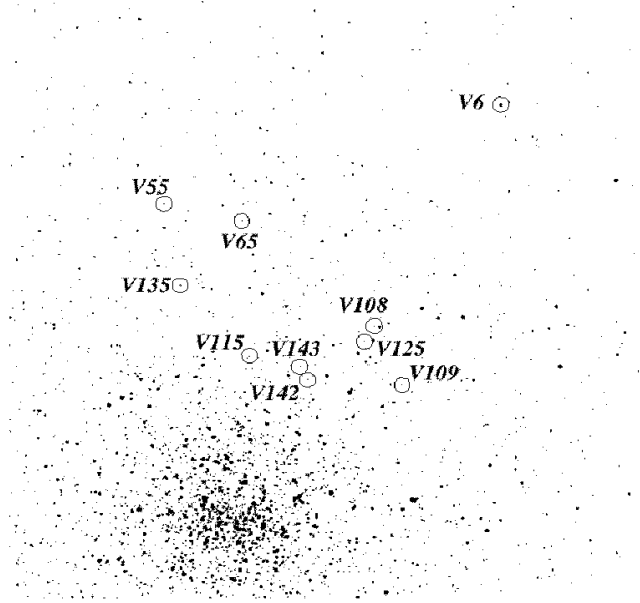


FIG. 2E.— NGC 6441 finding charts marking all of the variable stars found in this paper. Figure 2a shows the full field-of-view for our observations. The image is 283-by-267 arcseconds at maximum extent, with a scale of 22 pixels per arcsecond. North is up and east is to the left.

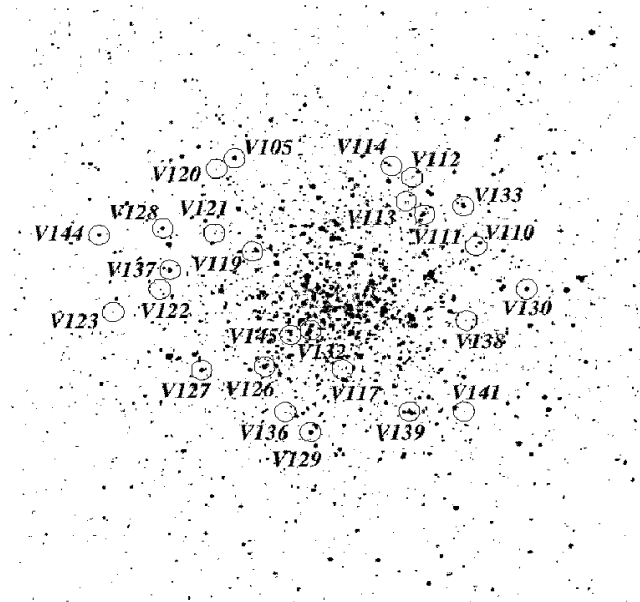


FIG. 2F.— NGC 6441 finding charts marking all of the variable stars found in this paper. Figure 2a shows the full field-of-view for our observations. The image is 283-by-267 arcseconds at maximum extent, with a scale of 22 pixels per arcsecond. North is up and east is to the left.

stars which produced light curves with significant scatter, and long period variables (LPVs) whose entire light cycle was not covered by our observations. We derived pulsation amplitudes and intensity-weighted magnitudes from the fitted templates. We estimate the uncertainty in these magnitudes to be 0.02–0.03 mag for the RRL stars and Population II Cepheid (P2C) stars. Typical uncertainties in the RRL and P2C periods are estimated to be 0.00002 and 0.002 days. The magnitude and period uncertainties are considerably larger for the LPV stars. In part, this is because the templates we used are not optimal for LPV stars, but a more significant discrepancy arises because many of the LPVs may not demonstrate pulsations with a regular period. The analysis here is intended only to classify the type of pulsa-

tion and to establish approximate mean-light parameters so the stars may be placed in the CMD. A comprehensive analysis of the LPV stars in NGC 6441 is reserved for a future paper.

Figure 3 shows the positions of the variables in the color-magnitude diagrams for NGC 6441 in  $V$  versus (a)  $B-V$  and (b)  $V-I$ , where variables are plotted according to their intensity-weighted  $\langle V \rangle$  magnitudes and  $\langle B \rangle - \langle V \rangle$  and  $\langle V \rangle - \langle I \rangle$  colors. Figures 3c and 3d give an expanded view of the HB. The variable stars along the HB are clearly RRL stars; those brighter than the HB and located toward the red but blueward of the red giant branch are P2Cs; those found after the turnover of the red giant branch are LPVs. However, as noted above, a number of the LPVs have poor periods due to aliasing and have larger un-

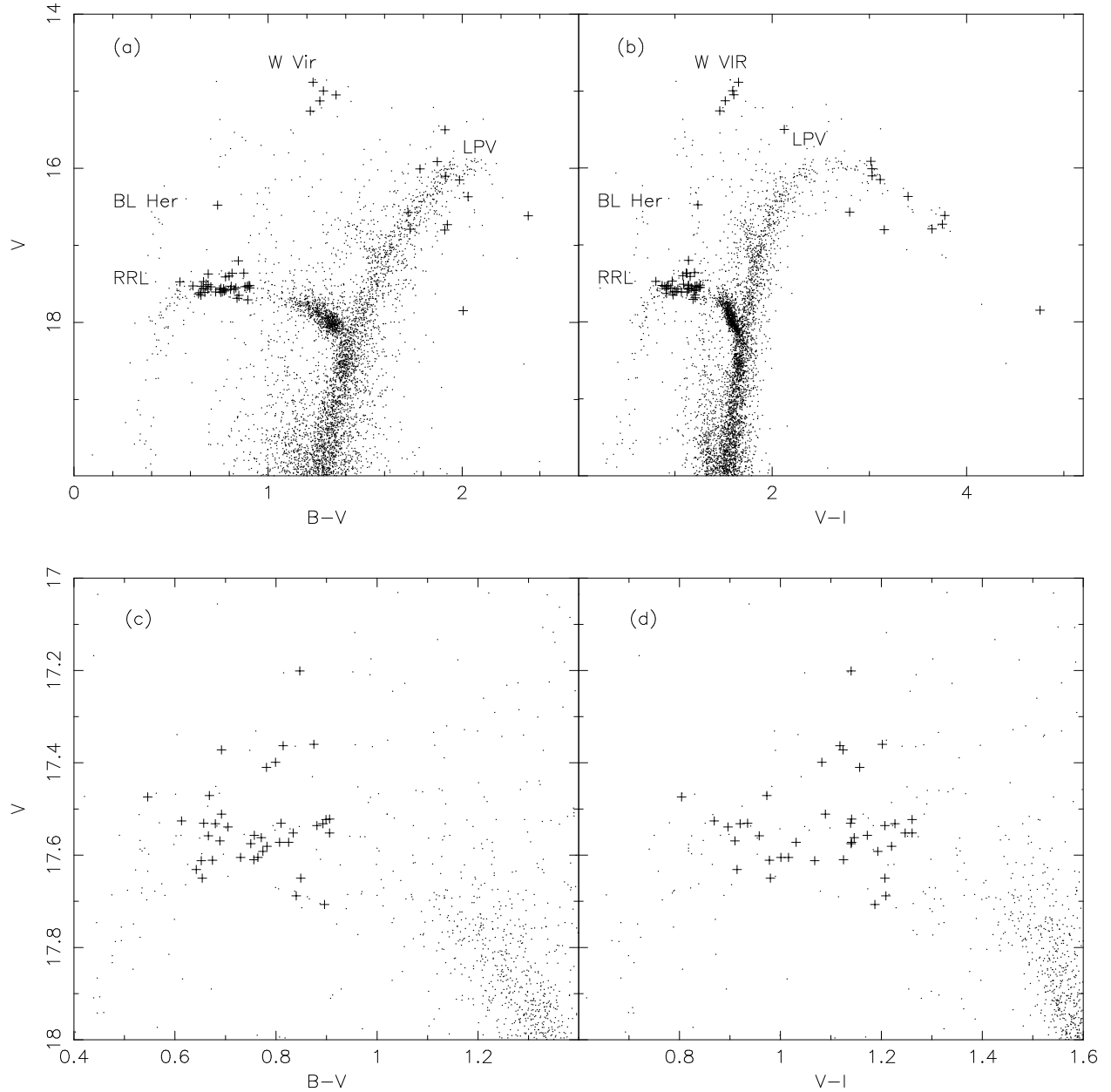


FIG. 3.— NGC 6441 color-magnitude diagram showing the location of the variable stars (pluses) found in this survey. The top two plots (a & b) show those found along the horizontal branch are clearly the RR Lyrae stars, while those found brighter than the horizontal branch are the Population II Cepheids. Those variables along the red giant branch are the long period variables. As noted in the text, these have uncertain magnitudes due to the method by which we calculated them. In the bottom two plots (c & d) we show a close-up of the horizontal branch. Here we see a number of candidate RR Lyrae stars are brighter than the majority of the RR Lyrae stars along the horizontal branch. These stars may be evolved RR Lyrae stars, while the brightest of these, V118, may be a Population II Cepheid.

certainties in their mean magnitudes. We also found one  $\delta$  Scuti star (V95), but given its magnitude it is likely a member of the field. Due to the small number of data points and the gaps in the phase coverage, we did not attempt to do a Fourier analysis of the light curves.

In the next sections we present the detailed results of our survey for variable stars and discuss their properties. Comparisons are also made to the variables found in ground-based surveys to determine any similarities and differences in their properties as compared to those found in this study.

### 3. RR LYRAE STARS

We were able to find 38 candidate RRL stars in the inner region of NGC 6441, with 24 of them being new. Previous

ground-based surveys (Layden et al. 1999; Pritzl et al. 2001) of the cluster found another 25 RRL stars which are not included in the field coverage of the present study. We also confirmed the variability of three stars whose variability had been suspected, but not confirmed. Thus, the total number of RRL stars known in NGC 6441 with definite classification and membership is now 63. Figure 4 shows the light curves of the 57 variables we identified where Layden’s template-fitting routines were used to fit the data. Tables 2, 3, and 4 list the  $B, V, I$  photometric data for the variable stars. The mean properties of the variable stars are given in Table 5. The mean periods for the 26 fundamental (RRab) and 12 RRL stars found in this survey are 0.753 d and 0.365 d, respectively. These values match up very well with those found from the ground-based surveys, which

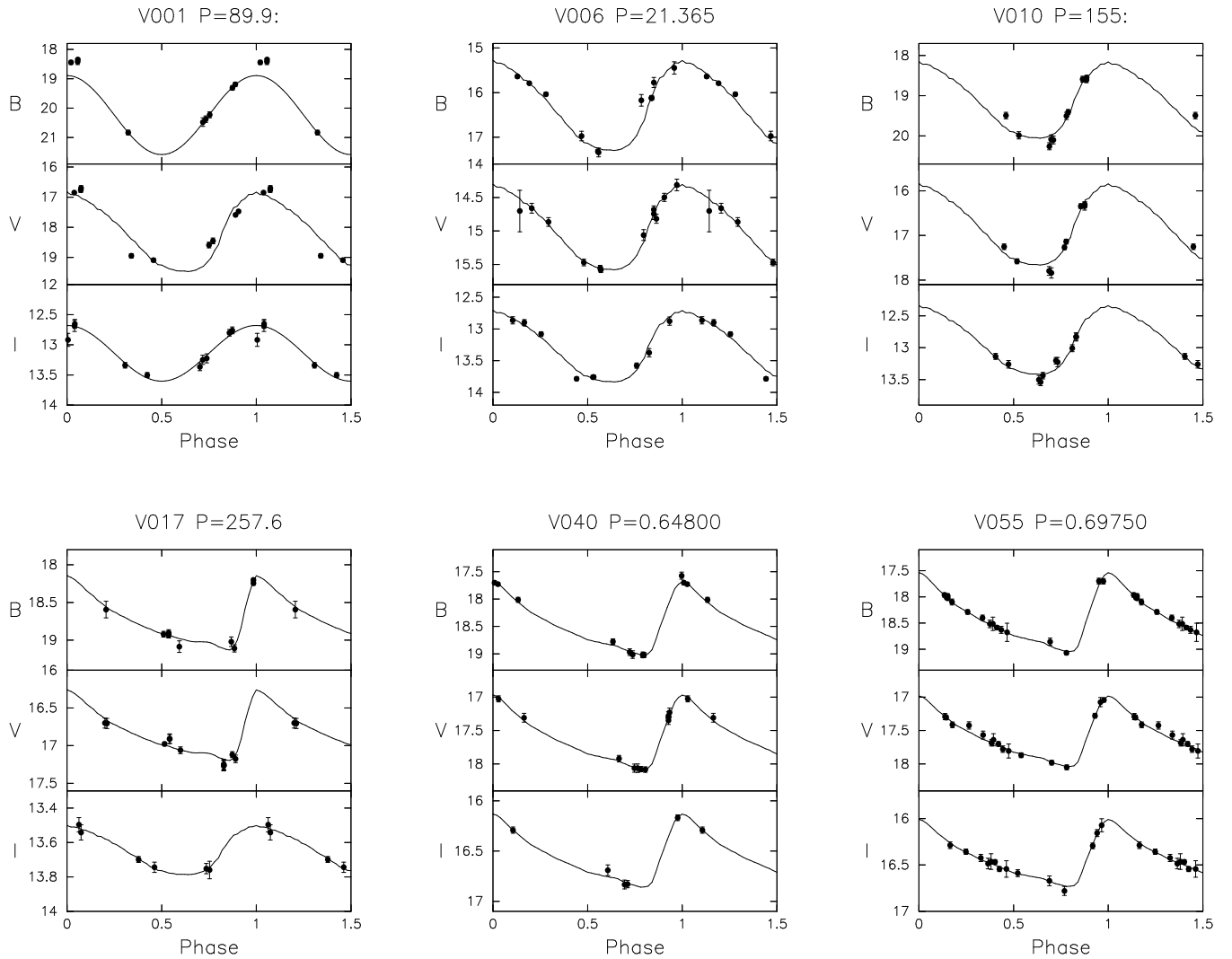


FIG. 4.— NGC 6441 light curves in  $B$ ,  $V$ , and  $I$ . Lines shown are template fits to the data. In some cases, mostly with the  $I$  data, the template was not able to find a good fit due to the quality of the data. Long period variables do not have good fits since the templates were not created to deal with this type of variable.

were  $\langle P_{ab} \rangle = 0.75$  d and  $\langle P_c \rangle = 0.38$  d for 24 and 9 stars, respectively (Pritzl et al. 2001). The variables listed in Table 5 from V55 to V102, were included in both the ground-based and HST surveys, so that the two samples are not completely independent. Combining the periods of the RRL stars with good light curves, accurate classifications, and certain membership found in this survey and the ground-based survey, we find the average periods for 42 RRab and 21 RRc stars in NGC 6441 to be 0.759 d and 0.375 d, respectively. The ratio of RRc to RRL stars is 0.33. As noted in Pritzl et al. (2000, 2001), the mean period of the RRab stars is higher than that found in the typical Oosterhoff II cluster. The mean period of the RRc stars is similar to that for Oosterhoff II clusters, while the  $N_c/N_{RR}$  ratio is somewhere between the values found for Oosterhoff I and II clusters.

Considering only the RRab stars newly discovered in this survey, we find a mean period of 0.765 d. This is slightly larger than one might expect given the result from the ground-based surveys (Layden et al. 1999; Pritzl et al. 2001). Since the HST observations allowed us to better survey the inner region of NGC 6441, it may be that there is a difference between the mean properties of the RRL in the inner and outer regions.

To make a more quantitative argument, we find the RRab stars within 20 arcsec of the cluster center to have a mean period of 0.766 d (17 RRab stars). Those outside this assumed radius have a mean period of 0.754 d (25 stars). The radius of 20 arcsec was chosen as the best to illustrate the difference in mean period. For radii less than this we begin to enter small-number statistics and for more than this the mean periods progressively get closer to matching.

Another way to view the shift in period is shown in Figure 5. The histogram in Fig. 5a illustrates that the distribution of RRL stars in NGC 6441 is closer to that of an Oosterhoff II cluster than that of an Oosterhoff I cluster, as discussed in Pritzl et al. (2000, 2001). A comparison of Fig. 5b and 5c shows an excess of longer period RRab stars within 20 arcsec of the cluster center. Some caution must be exercised, however, before one can conclude that the difference is real. A two-sample K-S test run on the inner and outer RRab results in a  $D$  statistic of 0.2259, which means that the two distributions are the same at a 62.1% confidence level. A Student  $t$ -test, which specifically tests if two distributions are different based on their means, was also run and resulted in a  $t$  value of 0.411, which means that the two distributions are indistinguishable at a 68.3% confidence level.

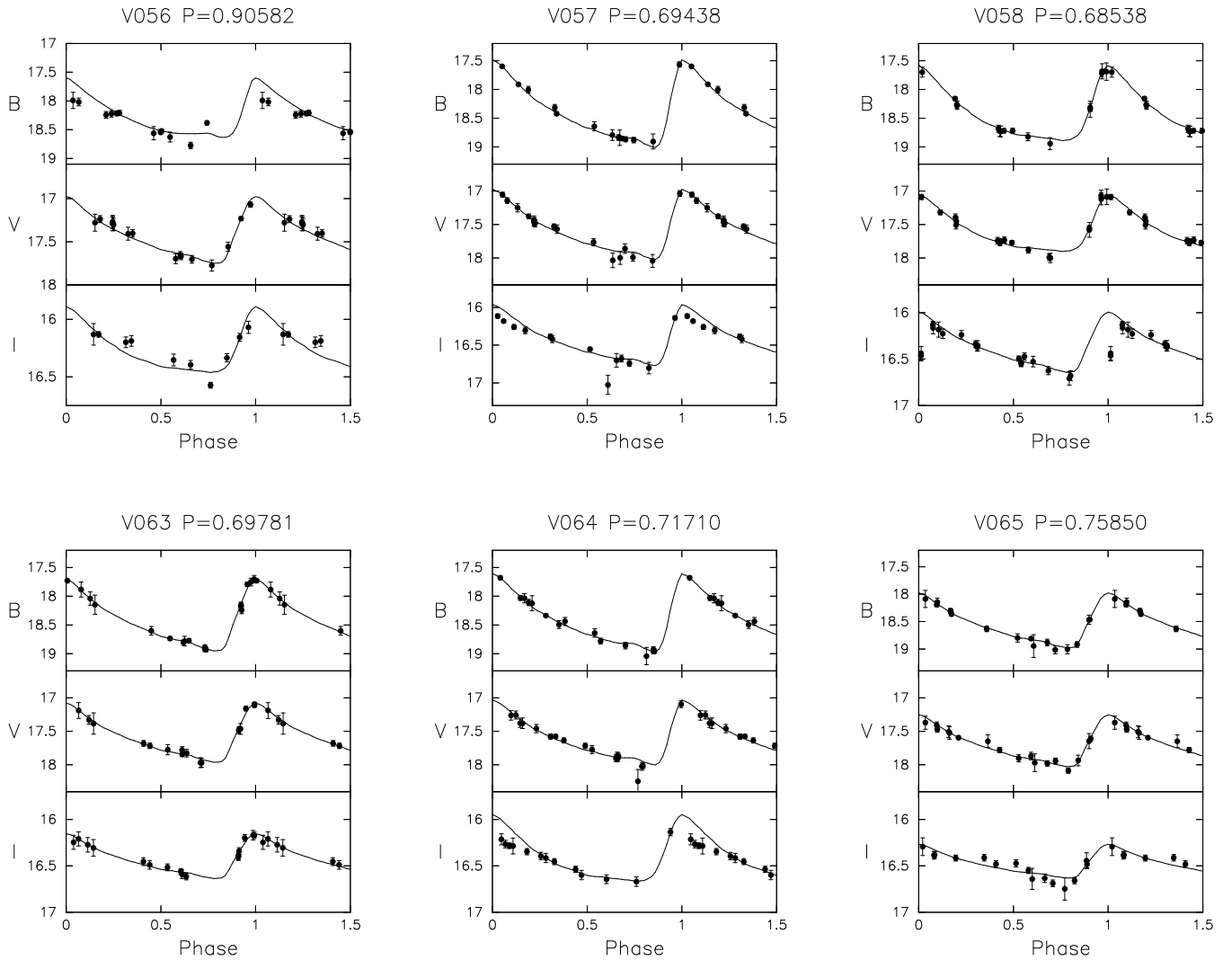


FIG. 4 CONT.— NGC 6441 light curves in  $B$ ,  $V$ , and  $I$ . Lines shown are template fits to the data. In some cases, mostly with the  $I$  data, the template was not able to find a good fit due to the quality of the data. Long period variables do not have good fits since the templates were not created to deal with this type of variable.

This confirms the K-S test, thus suggesting that the two samples are not significantly different, in a statistical sense. While our HST observations have been able to survey the inner regions of NGC 6441, crowding in the regions just outside this survey area may have prevented low amplitude, long period RRab stars from being detected in the ground-based surveys. As an example, adding five stars with periods of 0.85 d outside 20 arcsec would change the mean period to match that found for the RRab inside 20 arcsec. We also note that if V118 is truly a P2C (see §4) and not an evolved RRL star, the mean period for the RRab stars within 20 arcsec would be 0.753 d. This matches up very well with the mean period for the RRab stars outside 20 arcsec and argues that there may be no significant difference between the RRab populations inside and outside 20 arcsec. Further observations of NGC 6441 with better resolution at larger radii may help clear up any distinctions between the inner and outer RRab stars. Alternately, application of the ISIS image subtraction package (Alard 2000) may improve the detection of low amplitude variables in the crowded regions of NGC 6441 observed from the ground. We did not discuss the RRc stars given their relatively low numbers.

We derive the mean magnitude for the RRL stars to be

$m_{V,RR} = 17.54 \pm 0.02$  mag, where the error is the standard deviation of the mean. This matches up well with what was found in the ground-based survey of Pritzl et al. (2001;  $m_{V,RR} = 17.51 \pm 0.02$  mag). As seen in Figure 3, a number of the candidate RRL stars are found at magnitudes brighter than the majority of the RRL stars. These variable stars have periods of 0.90582 d (V56), 0.76867 d (V110), 0.61419 d (V112), 0.97923 d (V118), 0.80573 d (V136), and 0.55581 (V145). It may be that differential reddening is playing a role given that there is a small number of RRL stars fainter than the majority of the RRL stars. It has already been shown from the RRL star light curves that differential reddening affects the ground-based observations of NGC 6441 (Layden et al. 1999; Pritzl et al. 2001). We did not attempt to determine the reddenings from the RRab stars in this survey via their  $B-V$  color at the minimum (Blanco 1992) due to the small number of data points. It may also be the case that some of these stars have evolved further from the zero-age HB and are thus more luminous. The periods for two of the stars, V118 (and, to a lesser extent V56) and V145, are long for RRab and RRc stars, respectively. In fact, given the magnitude and the period of V118, it may be the faintest P2C in the cluster (see §4).



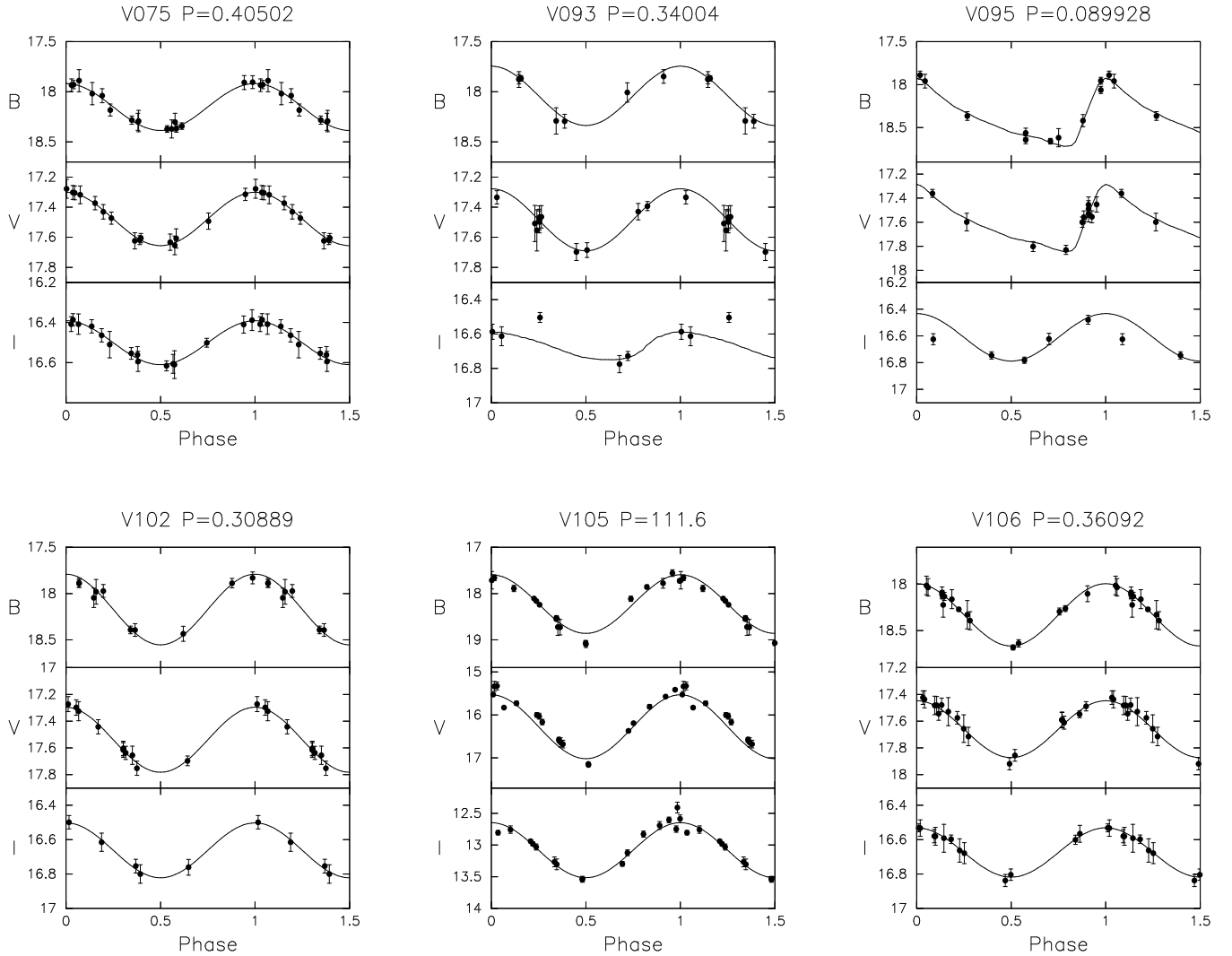


FIG. 4 CONT.—NGC 6441 light curves in  $B$ ,  $V$ , and  $I$ . Lines shown are template fits to the data. In some cases, mostly with the  $I$  data, the template was not able to find a good fit due to the quality of the data. Long period variables do not have good fits since the templates were not created to deal with this type of variable.

### 3.1. Period-Amplitude Diagram

Figure 6 shows the period-amplitude diagrams for the newly discovered RRL stars and those previously found (Pritzl et al. 2001). In general, the RRL stars from the two data sets lie in the same regions of the diagrams. There is more of a spread among the RRab in Fig. 6c because the  $I$ -band light curves have more scatter than the  $B$  and  $V$  light curves. From Figure 6 we see that the general properties of the RRL stars found in the inner region of the cluster are the same as those found in the outer regions.

It was noted in Layden et al. (1999) and Pritzl et al. (2001) that some of the RRab stars were likely blended with other stars, producing lower than expected amplitudes for their periods. Such blends are likely given the compact nature of this cluster. The candidate blended stars from the ground-based surveys can be seen in Figure 6 as those RRab stars which are scattered toward lower amplitudes. In Table 6, we show the comparison between the variable stars found in both this survey and the ground-based survey of Pritzl et al. There are clearly a number of stars which appeared significantly brighter in the ground-based survey and had lower amplitudes than found in the present survey. We also examined the images for stars

neighboring those listed in Table 6. All of the stars listed which showed significant differences in their magnitudes and periods were found to have nearby stars that likely affected the photometry of the ground-based studies. The higher resolution of the WFPC2 indicates that the previous conclusion of the “low amplitude” RRab stars in the ground-based survey being blends was correct. There is also the possibility that some of these stars may be experiencing the Blazhko effect which also affects the amplitudes of RRL stars.

Layden et al. (1999) and Pritzl et al. (2000, 2001) found that the RRab stars in NGC 6441 lie at longer periods in the period-amplitude diagram compared to field RRab stars of similar metallicity. This confirms that the RRL stars, and therefore the HB, are unusually bright for their metallicity. Pritzl et al. (2001) also showed that the RRab stars in NGC 6441 fall near a line in the period-amplitude diagram established by Clement (2000) as defining the location of RRab stars in Oosterhoff type II clusters, a result first noted by Clement and reconfirmed here in Fig. 6b. As noted above, this is consistent with the mean period of the RRab actually being more like that of an Oosterhoff type II cluster than an Oosterhoff type I cluster (see also Walker 2000). As discussed in detail in Pritzl et al. (2002), it

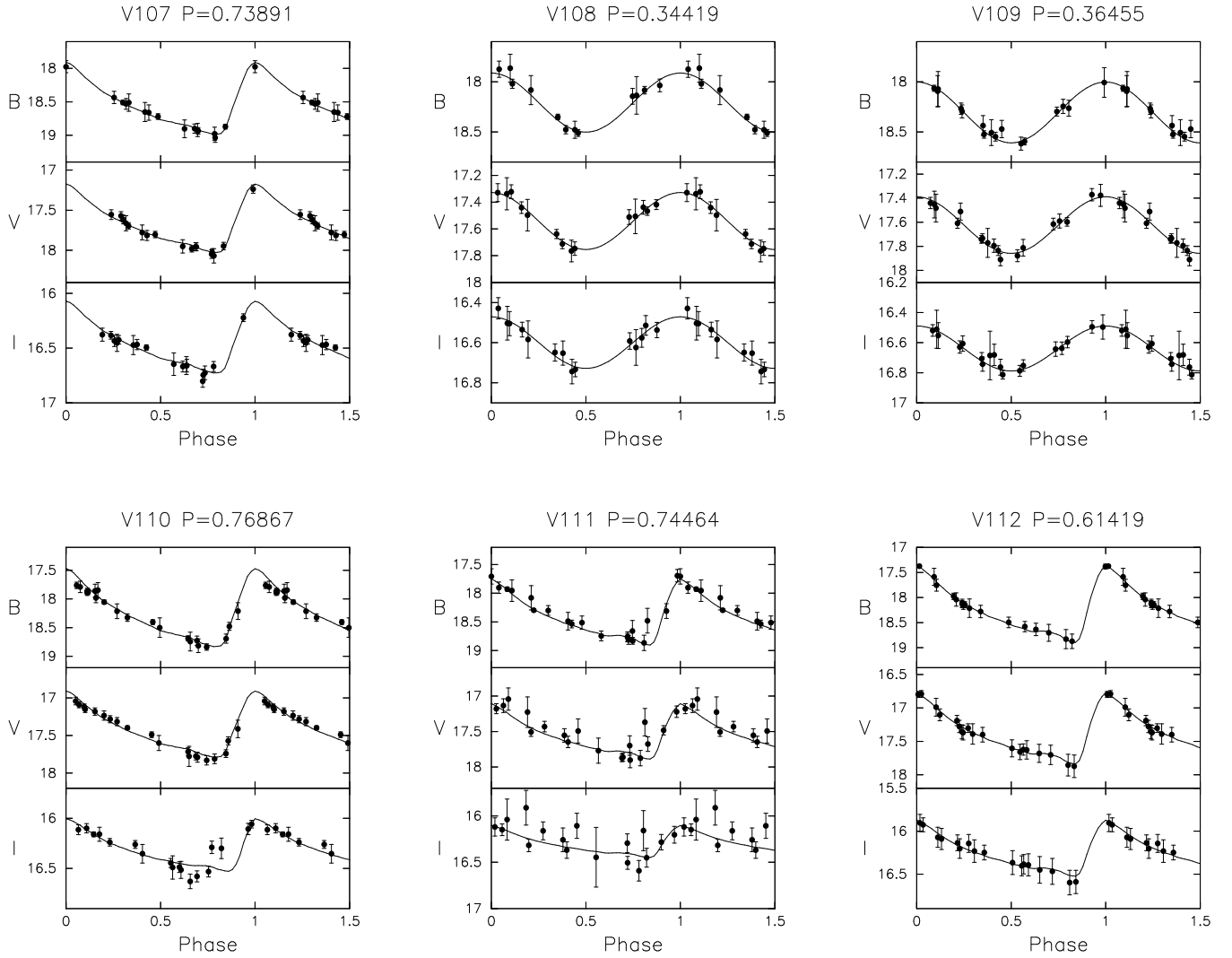


FIG. 4 CONT.— NGC 6441 light curves in *B*, *V*, and *I*. Lines shown are template fits to the data. In some cases, mostly with the *I* data, the template was not able to find a good fit due to the quality of the data. Long period variables do not have good fits since the templates were not created to deal with this type of variable.

is difficult to model such GCs as NGC 6388 and NGC 6441 as Oosterhoff II systems, under the hypothesis that their variables are evolved from a position on the blue zero-age HB, due to the small number of progenitors on the blue HB (see also Fig. 3).

We also find one RRc star of unusually long period in the inner region of NGC 6441 (V145). Two similarly long period RRc stars were found in the ground-based studies (Layden et al. 1999; Pritzl et al. 2001). In Figure 6 we see that most of the RRc stars group together, while the longer period ones are seen not to partake in the more usual, inverted parabola-like (e.g., Bono et al. 1997a) locus of RRc stars in the period-amplitude plane, for reasons which are still unclear. As noted for NGC 6441 in Pritzl et al. (2001), and for the long period RRc stars in NGC 6388 in Pritzl et al. (2002), there are very few GCs that produce this type of long period RRc star.

In Figure 6 we can also see that there are two candidate RRab stars with longer periods than expected for their amplitudes (V56 and V118). As noted above, these are two of the stars which are brighter than the majority of the other RRL stars. This prompts the question as to whether these stars are evolved RRL stars or possibly P2Cs. We will discuss the issue further in the following section.

### 3.2. *I*-band Period-Luminosity Relations

RRL stars provide excellent distance indicators given their nearly uniform absolute magnitudes. However, while the HB is flat at the RRL level in *B* and *V*, thus destroying any significant period-luminosity (P-L) relation that might otherwise be present due to the important range in  $T_{\text{eff}}$  compared to  $L$ , the same may not apply in redder (and bluer) bandpasses, where the HB becomes significantly non-horizontal at the RRL level. Many studies have been done to determine the *K*-band P-L relations for RRL stars (Longmore et al. 1990; Nemeč, Nemeč, & Lutz 1994; Bono et al. 2001). The RRL P-L relations in the *I*-band have, on the other hand, been neglected. We searched through the literature and found only Layden & Sarajedini (2003) derived a P-L relation in the *I*-band for the RRL in NGC 3201. Here we derive the *I*-band P-L relations for the RRL in NGC 6441 using the large number of RRL stars we found in this cluster.

As discussed here, in Layden et al. (1999), and in Pritzl et al. (2001, 2002), the RRL stars in NGC 6388 and NGC 6441 are unusually bright for their metallicity. Given that the general properties of the RRL stars in both of these clusters are more like Oosterhoff II clusters than Oosterhoff I, we as-

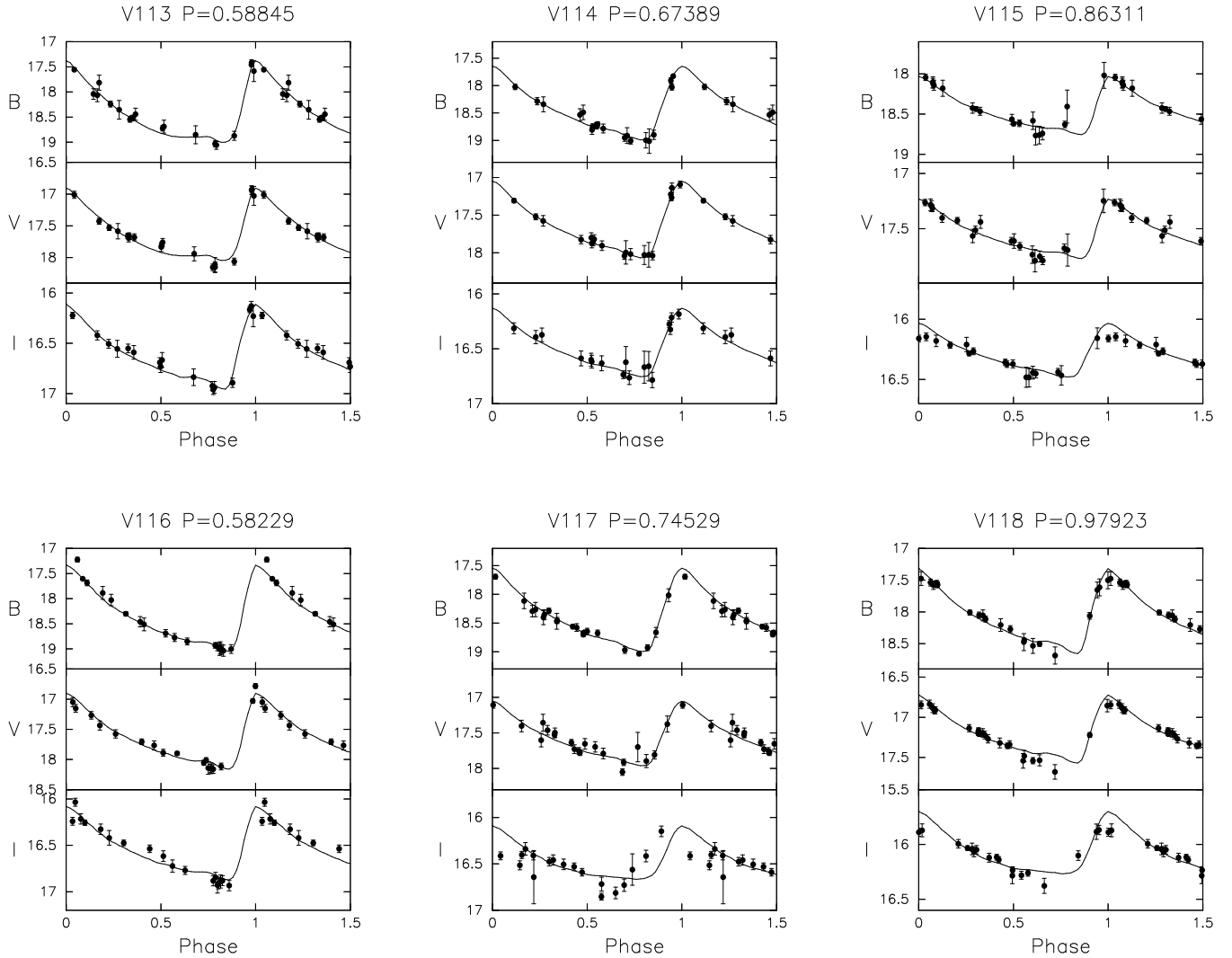


FIG. 4 CONT.— NGC 6441 light curves in *B*, *V*, and *I*. Lines shown are template fits to the data. In some cases, mostly with the *I* data, the template was not able to find a good fit due to the quality of the data. Long period variables do not have good fits since the templates were not created to deal with this type of variable.

sume that their RRL stars have absolute magnitudes similar to those of Oosterhoff II clusters such as M15. Using Eqn. 7 in Lee, Demarque, & Zinn (1990) and adopting a metallicity of  $[\text{Fe}/\text{H}] = -2.0$ , we find an absolute magnitude for the RRL stars in NGC 6441 to be  $M_V = +0.48$  mag. Our adopted magnitude for RRL stars in Oosterhoff Type II clusters is broadly consistent with the recent parallax determination for RRL stars by Benedict et al. (2002). They obtained  $M_V = +0.61$  for RR Lyrae itself, which, at  $[\text{Fe}/\text{H}] = -1.4$ , is more metal-rich and might be slightly fainter than RRL stars in a more metal-poor system. In calculating the distance modulus for NGC 6441, we adopt  $m_{V,RR} = 17.54$  mag,  $E(B-V) = 0.51$ , and  $R_V = 3.1$  to find  $\mu_0 = 15.48$  mag. To derive the individual absolute magnitudes we used  $A_I = 1.85E(B-V)$ . Figure 7 shows the P-L relations for the RRL stars. Removing outlying stars, we determine the P-L relations to be,

$$M_{I,ab} = -0.25(\pm 0.04) - 1.78(\pm 0.12) \log P \quad (1)$$

$$M_{I,c} = -0.61(\pm 0.06) - 1.78(\pm 0.14) \log P, \quad (2)$$

with correlation coefficients  $r = 0.792$  and  $0.947$ , respectively. The root-mean-square deviations for the RRab and RRLc relations are 0.06 and 0.04, respectively. As noted in §3, it is uncer-

tain whether the outlying stars, which are brighter than the majority of RRL stars of similar period, are evolved or not. Still, it is clear that the *I*-band provides a good filter to derive P-L relations for the RRL stars. We note that the zero-point for the above relations is uncertain due to the fact that we have assumed that the RRL stars in NGC 6441 have the same luminosity as Oosterhoff II RRL stars with  $[\text{Fe}/\text{H}] = -2.0$ . The precise luminosity of the NGC 6441 RRL stars is not conclusively known given the unusual nature of its HB.

#### 4. POPULATION II CEPHEIDS

In the ground-based photometry we were able to find four candidate P2Cs in NGC 6388 (Pritzl et al. 2002), but none in NGC 6441 (Layden et al. 1999; Pritzl et al. 2001). At the time it seemed strange that in two clusters with such similar HB morphology and RRL star populations, one would contain P2Cs and the other would not. In this HST snapshot survey we have found six definite P2C candidates in NGC 6441. This makes NGC 6441, along with NGC 6388, the most metal-rich GC known to contain P2Cs. Interestingly, the P2Cs in both clusters have been found near the inner regions of the clusters, though this may reflect just the comparatively small population of P2C

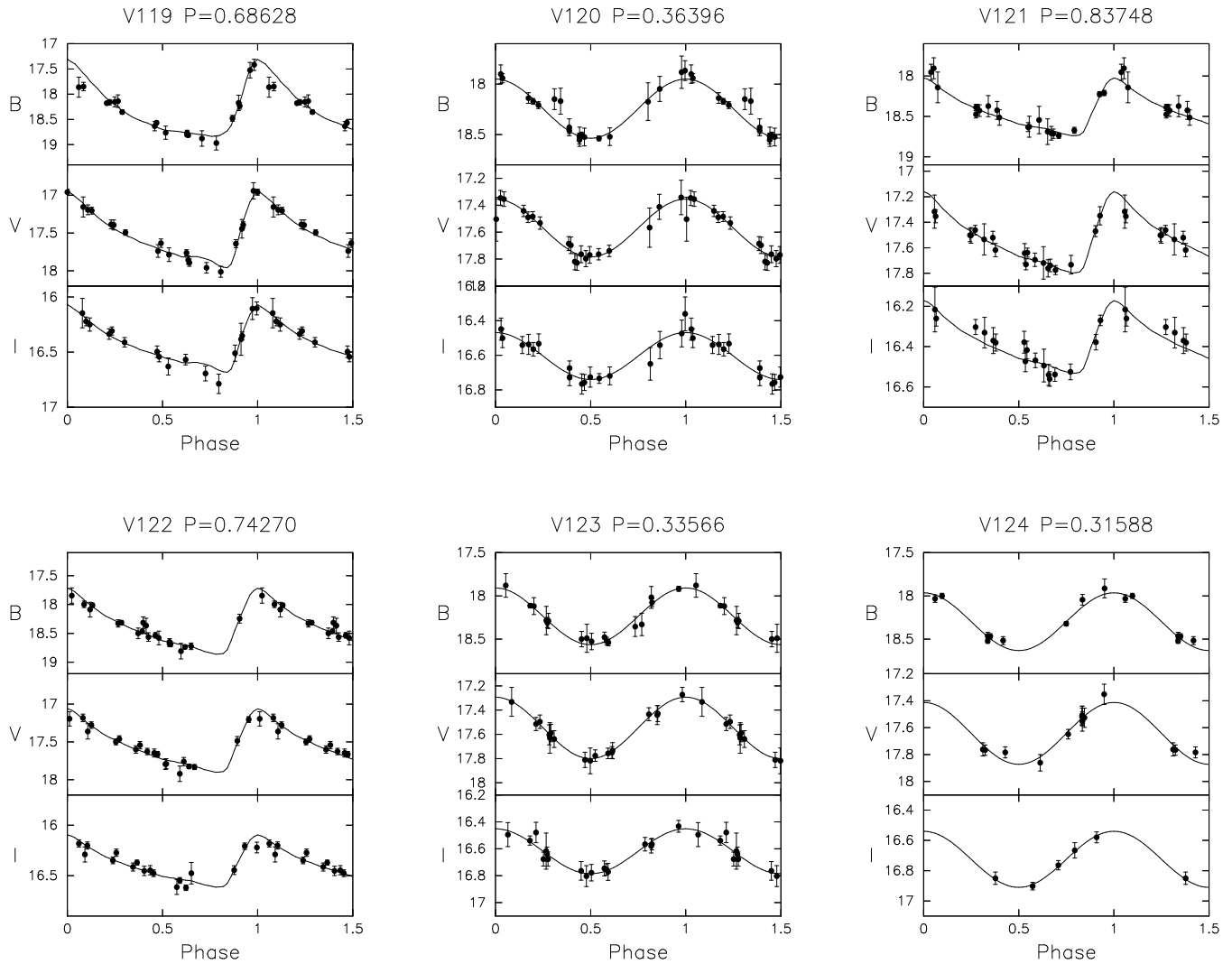


FIG. 4 CONT.—NGC 6441 light curves in *B*, *V*, and *I*. Lines shown are template fits to the data. In some cases, mostly with the *I* data, the template was not able to find a good fit due to the quality of the data. Long period variables do not have good fits since the templates were not created to deal with this type of variable.

stars compared to RRL variables. The discovery of P2Cs in these two clusters is consistent with the idea that these types of variables are found only in clusters with blue HB components (Wallerstein 1970; Smith & Wehlau 1985).<sup>9</sup>

Of the six P2Cs, five are of W Virginis type (W Vir;  $10 < P < 20$  d) and one is of BL Herculis type (BL Her;  $P < 10$  d). The difference between these types is not only defined by their periods, but also by their origins. As reviewed by Wallerstein (2002, but see also Bono et al. 1997b), BL Her stars are believed to derive from stars which have evolved from the HB bluer than the RRL gap, and which are now evolving redward through the instability strip at luminosities brighter than those of RRL stars. By contrast, W Vir stars, while also considered to be the progeny of blue HB stars (e.g., Gingold 1985), are believed to be undergoing helium shell flashes leading them along blueward loops into the instability strip as they move up the asymptotic giant branch (AGB). This is consistent with studies of period changes in P2Cs in GCs. Wehlau & Bohlender (1982) found that of 12 BL Her stars in Galactic GCs, nine had increasing periods, three had unchanging periods, and zero had decreasing periods. Increasing periods are expected for vari-

ables evolving redward from the blue HB toward the AGB. For the W Vir stars the picture is not so clear, but Clement, Hogg, & Yee (1988) found that a number of W Vir stars showed both increases and decreases in period, and that at least two variables showed long term period decreases consistent with blueward evolution. The period change observations for W Vir stars are thus at least consistent with evolution of W Vir stars into and out of the instability strip during blueward loops.

#### 4.1. Period-Luminosity Relation for Population II Cepheids

Given the relatively large number of P2Cs found in both NGC 6441 and NGC 6388, we would like to determine the P-L relations for these stars. We use the distance modulus derived in §3.2 for NGC 6441,  $\mu_0 = 15.48$  mag, to derive the absolute magnitudes for the P2Cs found in this survey. For NGC 6388, we follow the prescription used for NGC 6441 to derive its distance modulus. Since we assume that the RRL stars in NGC 6388 are of a similar nature as those in NGC 6441, we adopt the same absolute magnitude for its RRL stars,  $M_V = +0.48$  mag.

In Table 7 we list the data for the P2Cs in NGC 6388 and

<sup>9</sup> Palomar 3 is a notable exception to this otherwise seemingly general rule (Borissova, Ivanov, & Catelan 2000).

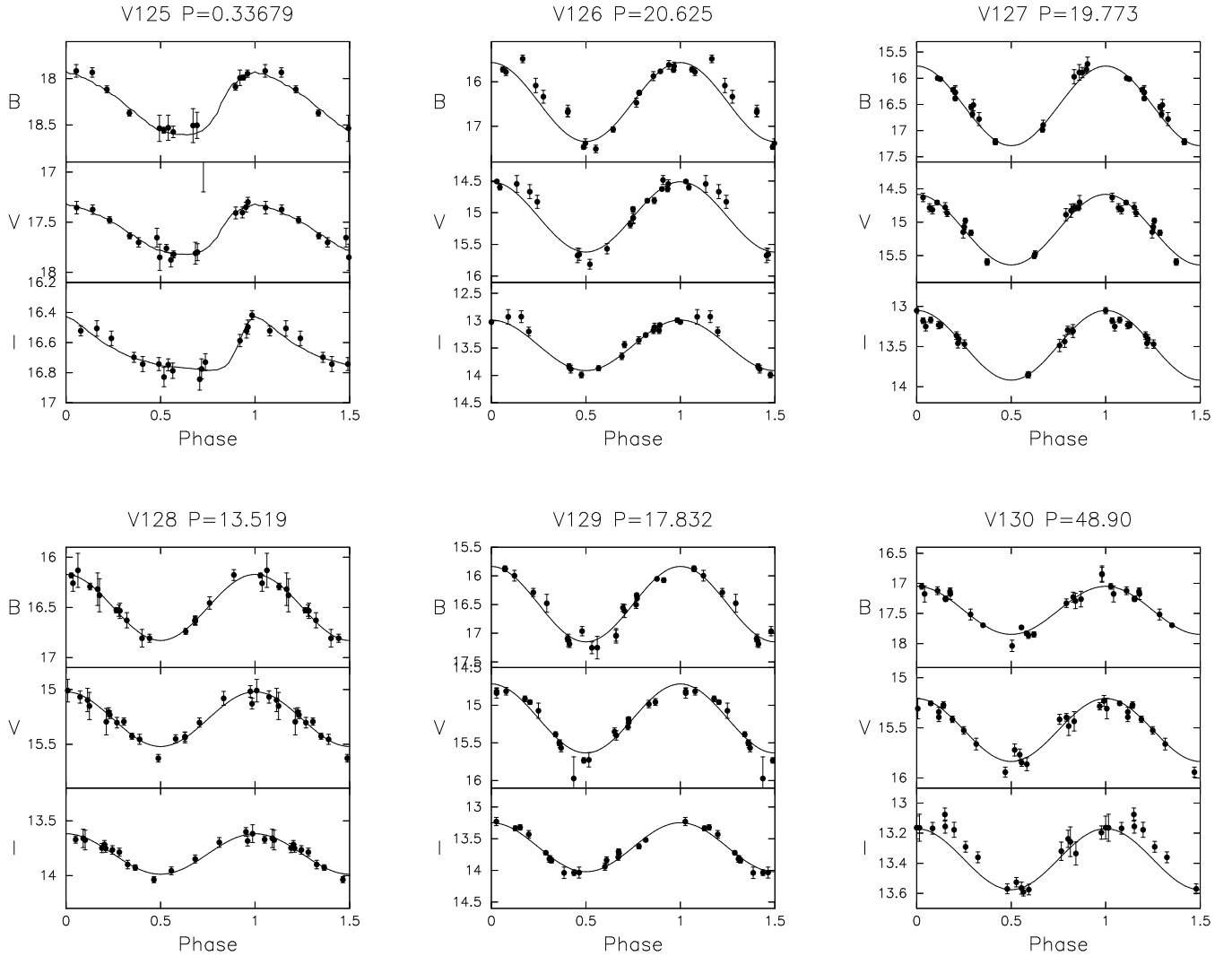


FIG. 4 CONT.—NGC 6441 light curves in  $B$ ,  $V$ , and  $I$ . Lines shown are template fits to the data. In some cases, mostly with the  $I$  data, the template was not able to find a good fit due to the quality of the data. Long period variables do not have good fits since the templates were not created to deal with this type of variable.

NGC 6441. For our discussions here, we will include V118 with the P2Cs, although its precise classification is uncertain. We have chosen not to include V56 since its period and magnitude are not unreasonably different from the other RRL stars. We have assumed  $R_V = 3.1$ ,  $R_B = 4.1$ , and  $A_I = 1.85E(B-V)$ , and have adopted mean reddenings of  $E(B-V) = 0.40 \pm 0.03$  and  $0.51 \pm 0.02$  for NGC 6388 and NGC 6441, respectively (Pritzl et al. 2001, 2002). Figure 8 shows the absolute magnitudes of the P2Cs in NGC 6388 and NGC 6441 for the various filters. In each panel of Figure 8, we see that the P2Cs form a surprisingly good correlation from shorter to longer periods, with the lone exception of one star in NGC 6388. V29 of NGC 6388 was shown to be unusually bright for its period in Pritzl et al. (2002) leading to the idea that it may be blended with another star. Leaving that star out, we determined the following P-L relations,

$$M_V = 0.05(\pm 0.05) - 1.64(\pm 0.05) \log P \quad (3)$$

$$M_B = 0.31(\pm 0.09) - 1.23(\pm 0.09) \log P \quad (4)$$

$$M_I = -0.36(\pm 0.01) - 2.03(\pm 0.03) \log P, \quad (5)$$

with correlation coefficients  $r = 0.996$ ,  $0.985$ , and  $0.998$ , respectively. The root-mean-square deviation for each relation

is  $0.07$ ,  $0.10$ , and  $0.06$  for  $V$ ,  $B$ , and  $I$ , respectively. Both the slopes for  $M_V$  and  $M_B$  match up quite well with those found by McNamara (1995, Eqns. 11 and 12) for P2Cs with periods less than ten days, but are very different compared to the results of Alcock et al. (1998, Eqn. 5) for longer period P2Cs. The tight fits to the relations also indicate that all of the P2Cs in NGC 6388 and NGC 6441 are likely to be pulsating in one mode, presumably the fundamental mode. Following the suggestion by Alcock et al. that adding a color term results in better relations, we calculated the P-L-C relations for the NGC 6441 and NGC 6388 P2Cs and found no significant improvement in the quality of the fit. This may be explained by the already excellent correlation of the P2Cs in the P-L relations and the fact that Alcock et al. found the RV Tauri (RV Tau;  $P > 20$  days) benefited the greatest in adding in the color term.

#### 4.2. Comparison of Period-Luminosity Relations

Defining a clear P-L relation is important in the use of Cepheid variable stars in distance determinations. While other Cepheid-type variables such as the classical and anomalous types have their P-L relations well-defined, the relations for the

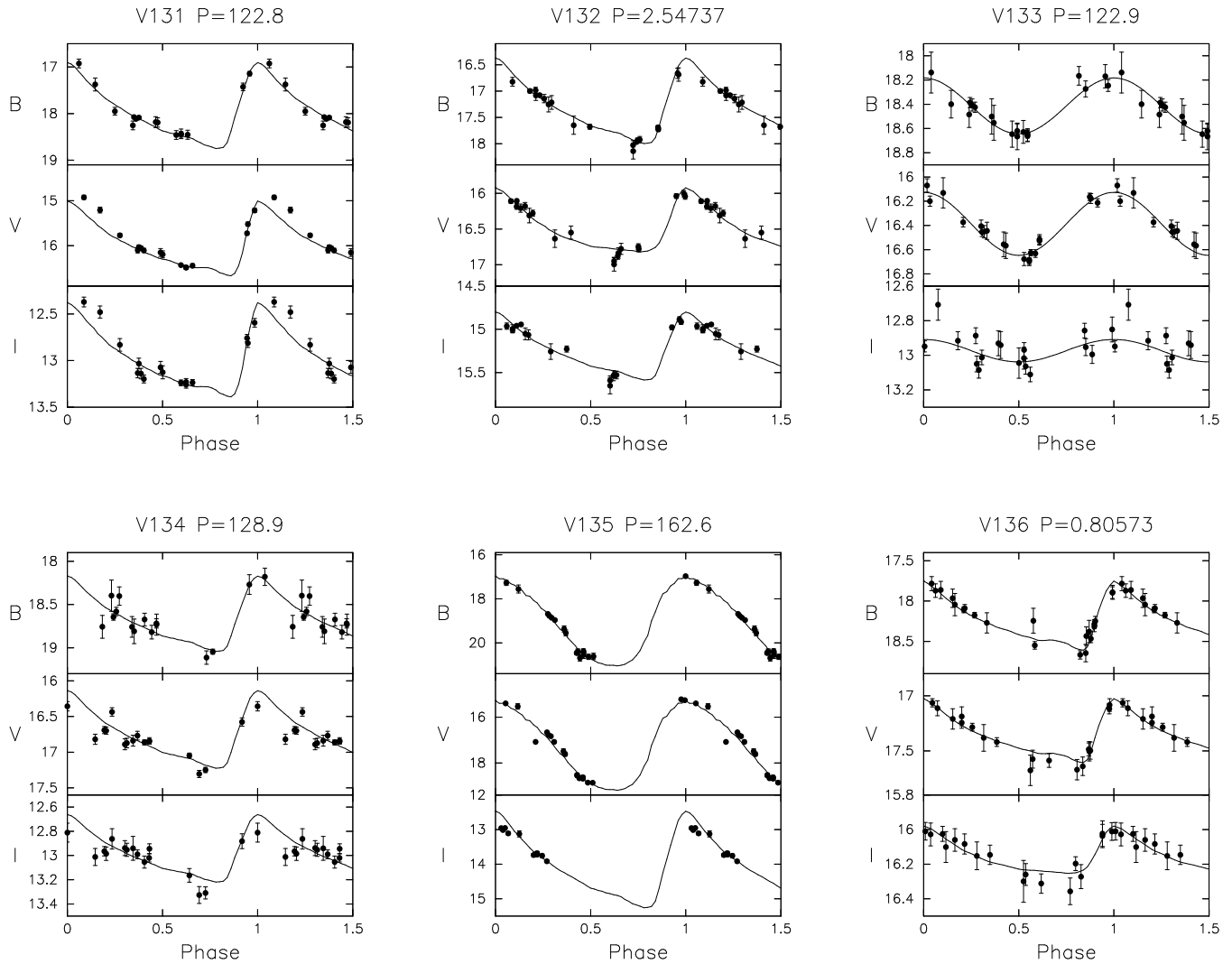


FIG. 4 CONT.— NGC 6441 light curves in *B*, *V*, and *I*. Lines shown are template fits to the data. In some cases, mostly with the *I* data, the template was not able to find a good fit due to the quality of the data. Long period variables do not have good fits since the templates were not created to deal with this type of variable.

P2Cs in general are still somewhat uncertain. Arp (1955a) argued that P2Cs follow at least two parallel P-L relations, one each for fundamental and overtone mode pulsators. Others later favored a single P-L relation to describe the P2Cs (e.g., Dickens & Carey 1967; Demers & Harris 1974). Harris (1985) also assumed a single P-L relation, but with a break toward a steeper slope for P2Cs with periods greater than 12.5 days. The theoretical *B*-band P-L relations of Bono et al. (1997b) show a break in slope near  $P = 15$  days at the faint boundary of the domain in which P2Cs might exist, but no break in slope at the brighter boundary.

In their paper on Population II variable stars, Nemeč, Nemeč & Lutz (1994) revived Arp's model stating that P2Cs are pulsating in either fundamental or first overtone modes, which followed their theme that all pulsating variable stars can be found to have both pulsation modes. However, McNamara (1995), using the data from Nemeč et al., stated that the observations were better fit by one line describing the BL Her stars ( $P < 10$  d) and another fitted to the W Vir stars ( $P > 10$  d), similar to what was argued by Harris (1985). Recently, Alcock et al. (1998) used a sample of 33 P2Cs in the Large Magellanic Cloud (LMC) in the period range of  $0.9 < \log P < 1.75$  to compare the various P-L

relations. While noting that the Galactic GC P-L relations provided adequate fits to the shorter period LMC P2Cs, they found that those P-L relations did not provide a good fit for the longer period RV Tau stars, which appear more luminous than the P-L relations predicted. Combining the Galactic GC and LMC data sets, Alcock et al. found that the shorter period Galactic GC P2Cs provided a good linear extension to the LMC data with the RV Tau stars turning toward brighter magnitudes. To account for this, Alcock et al. included a color term to their P-L relations for  $\log P > 0.9$ , which greatly reduced the scatter in the data and the up-turn of the RV Tau stars. They concluded that the RV Tau stars are direct extensions of the other P2C types. Unfortunately, the Alcock et al. data were taken with *V* and *R* filters, while most of the Galactic GC data is in *B* and *V*. This makes the application of their P-L-C relation difficult to apply to other data sets.

To help clarify the issue of the differing slopes found by various studies, we investigated the P2Cs in other GCs and incorporated them in our analysis. Table 8 lists the properties of the Galactic GC P2Cs summarizing the data found in the literature. We estimated the absolute magnitudes for each star using Eqn. 7 of Lee et al. (1990) and the metallicities, reddenings, and  $V_{\text{HB}}$

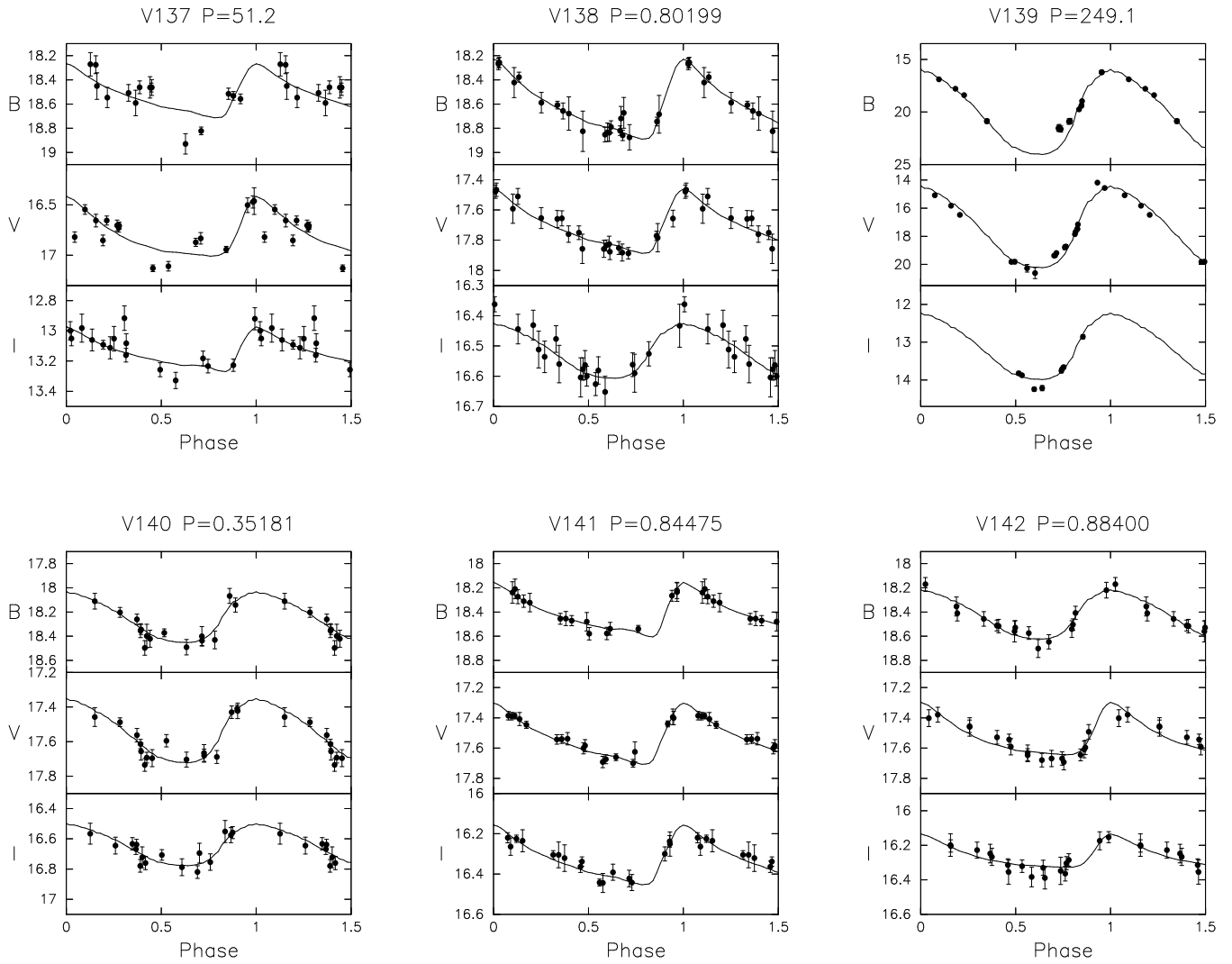


FIG. 4 CONT.— NGC 6441 light curves in *B*, *V*, and *I*. Lines shown are template fits to the data. In some cases, mostly with the *I* data, the template was not able to find a good fit due to the quality of the data. Long period variables do not have good fits since the templates were not created to deal with this type of variable.

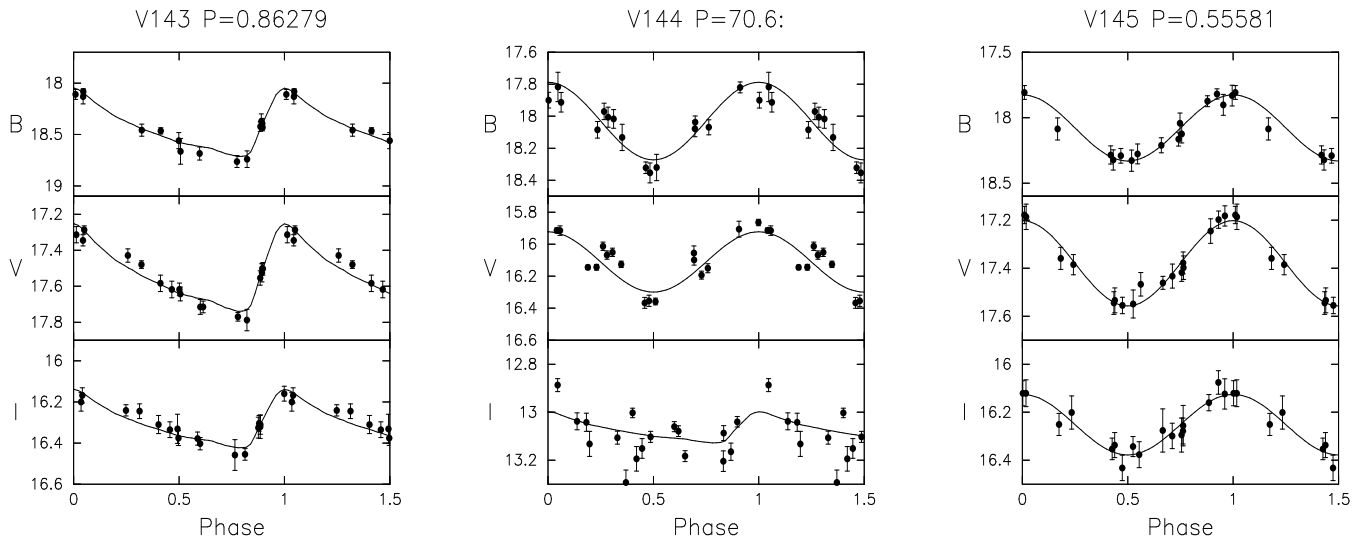


FIG. 4 CONT.— NGC 6441 light curves in *B*, *V*, and *I*. Lines shown are template fits to the data. In some cases, mostly with the *I* data, the template was not able to find a good fit due to the quality of the data. Long period variables do not have good fits since the templates were not created to deal with this type of variable.

given in Harris (1996). The format is the same as in Table 7. We plot the best available data for the Galactic GC P2Cs in

the top row of Figure 9, including those found by Alcock et al.

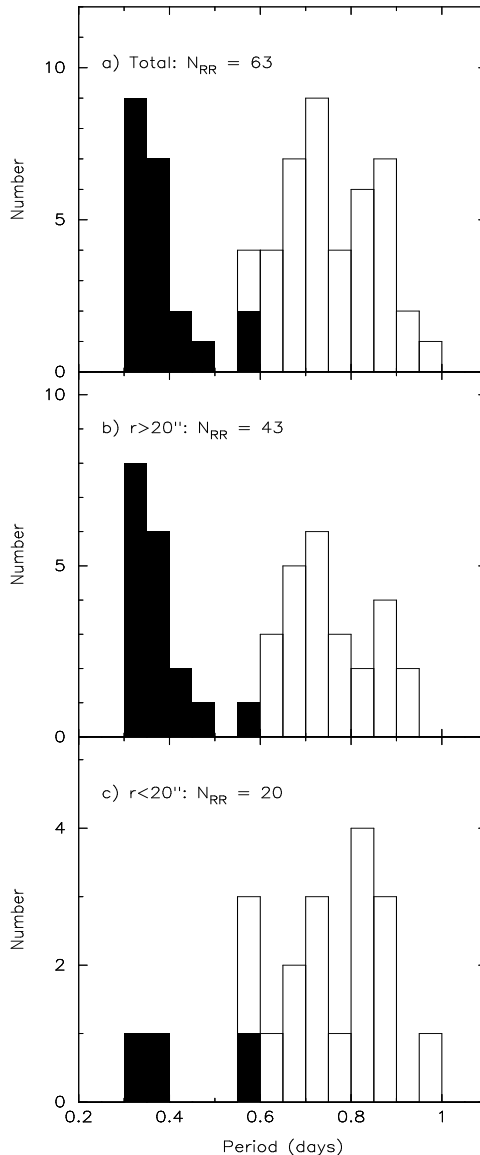


FIG. 5.— NGC 6441 RR Lyrae histograms for a) all known RR Lyrae, b) those outside 20 arcsec, and c) those within 20 arcsec. The filled bars represent the RRc stars, while the unfilled ones are the RRab stars. In (a) we see that NGC 6441 has the typical Oosterhoff Type II distribution with a higher proportion of RRc-to-RRab stars as compared to Oosterhoff Type I clusters whose RR Lyrae populations are primarily RRab stars. There is a small shift toward longer period for the RR Lyrae inside 20 arcsec.

(1998) in the LMC where they adopted a distance modulus of 18.5 mag. The only P2Cs not included in the plot were those from NGC 4372, which are clearly too faint. The periods listed for these stars may be correct, but the faint magnitudes may be due to the fact that Kaluzny & Krzeminski (1993) were searching for contact binaries and SX Phoenicis stars resulting in the candidate P2Cs being saturated. There is some scatter among the P2Cs in Fig. 9a, which is to be expected since it is known that there is some width to the instability strip. Fig. 9b shows a lot of scatter which may possibly be attributed to the presence of older photographic data, as compared to the  $I$  data in Fig. 9c which is only from CCD data. We plot in the bottom row of Figure 9 only those P2Cs with CCD photometry, except again for NGC 4372. This helps to reduce the scatter, as seen in Fig. 9d, but some still remains. Without any color information we are not able to tell if this scatter may be intrinsic, possibly due to the width of the P2C instability strip, or if it is photometric. It should be noted that the scatter seen at shorter periods in Fig. 9d

can be attributed to the  $\omega$  Cen P2Cs, a number of which have poor light curves (Kaluzny et al. 1997). For  $B$  and  $I$ , the CCD data are mostly taken from this study, but it is encouraging that the other data are consistent with what we have found.

Taking a closer look at the  $B$  and  $I$  data, it does not look like there is a change in the slope between the BL Her and W Vir stars. However, this is a tentative conclusion given the fact that most of the data comes from this survey alone. If we examine the  $V$  data in Fig. 9d, where more points are available, we can make some stronger arguments. There is clearly a change in the slope toward brighter magnitudes at longer periods. The question is whether this change is found at or around 10 or 12 days as suggested by Harris (1985) and McNamara (1995) or at a longer period. If we consider only the BL Her and W Vir stars, there is statistically no change in the slope between the two groups of P2Cs. On the other hand, if we consider the RV Tau stars, they clearly have a different slope from that of the shorter period Cepheids. It appears, therefore, that a single P-L rela-



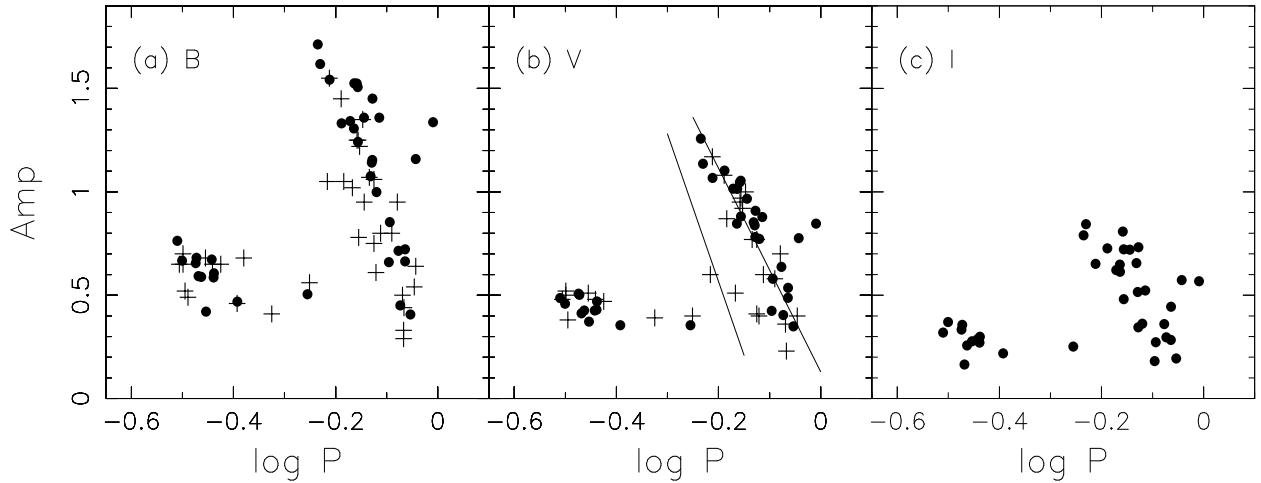


FIG. 6.— NGC 6441 period-amplitude diagrams for the RR Lyrae stars. RR Lyrae stars found in this survey are shown as filled circles, while those found in the ground-based survey of Pritzl et al. (2001) are shown as pluses. There are no clear differences between the RR Lyrae stars found in the inner and outer regions of NGC 6441. RRab stars in the ground-based survey scattered toward lower amplitude for their period were likely blended with other stars. The two lines shown in (b) represent the mean locus for the RRab stars in Oosterhoff I and Oosterhoff II globular clusters (Clement 2000). The NGC 6441 RRab stars fall nearer the Oosterhoff II line even though according to the metallicity of NGC 6441 it should be an Oosterhoff I cluster.

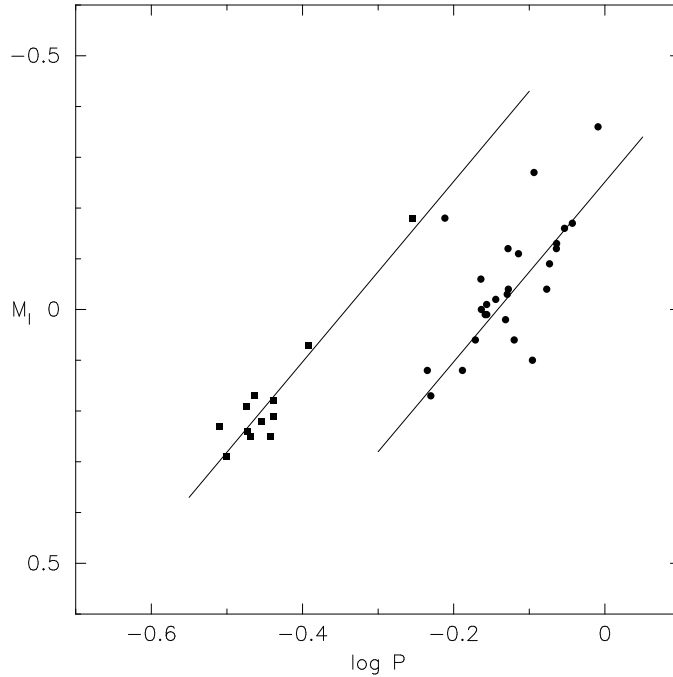


FIG. 7.— *I*-band period-luminosity plot for the RR Lyrae stars in NGC 6441. The lines shown were derived after excluding the outlying RR Lyrae stars.

tionship can be used to describe the P2Cs until periods greater than about 20 days are reached, when variables with RV Tau characteristics begin to enter the mix. Unfortunately, given the scarcity of data, we are not able to test the conclusion of Alcock et al. (1998) that adding in the color term to the RV Tau stars brings them more into line with the other P2C types.

Another possibility is raised by Fig. 9d. Alcock et al. (1998) identified a number of W Vir stars found in the LMC that are brighter than the bulk of the W Vir stars. These variables appear to constitute a straight line in combination with the brighter RV Tau stars that appears to be parallel to a line that could be drawn through the BL Her and W Vir stars. Alcock et al. (1998) classified their RV Tau stars as those having periods longer than 20 days. It may be that some of their W Vir stars are actually

RV Tau stars, and vice versa. There appears to be in reality no sharp dividing line between the W Vir and RV Tau stars, with the longest period W Vir variables gradually taking on RV Tau characteristics (Alcock et al. 1998).

At this point, it is uncertain how well the relations created from the NGC 6441 and NGC 6388 P2Cs apply to other GCs given the small amount of CCD photometry. Two of the more important questions are how good are the zeropoints we are using to derive the absolute magnitudes and is there any metallicity dependence in the relations which is currently not being taken into account in our relations. Clearly, more CCD photometry needs to be taken of P2Cs in order to clarify these issues, especially in the *B* and *I* filters, before any firm conclusions can be drawn.

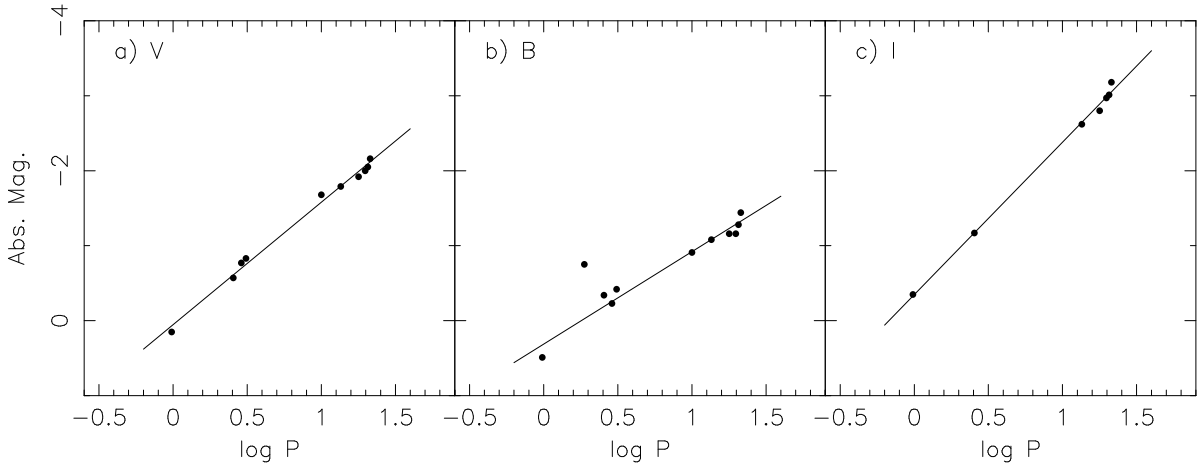


FIG. 8.— Period-luminosity plots for the Population II Cepheids in NGC 6441 and NGC 6388. All of the relations are shown to be exceptionally tight, with the exception of one star in *B* which is thought to be saturated (see text and Pritzl et al. 2002). The correlation coefficients are 0.985, 0.996, and 0.998 for *B*, *V*, and *I*, respectively.

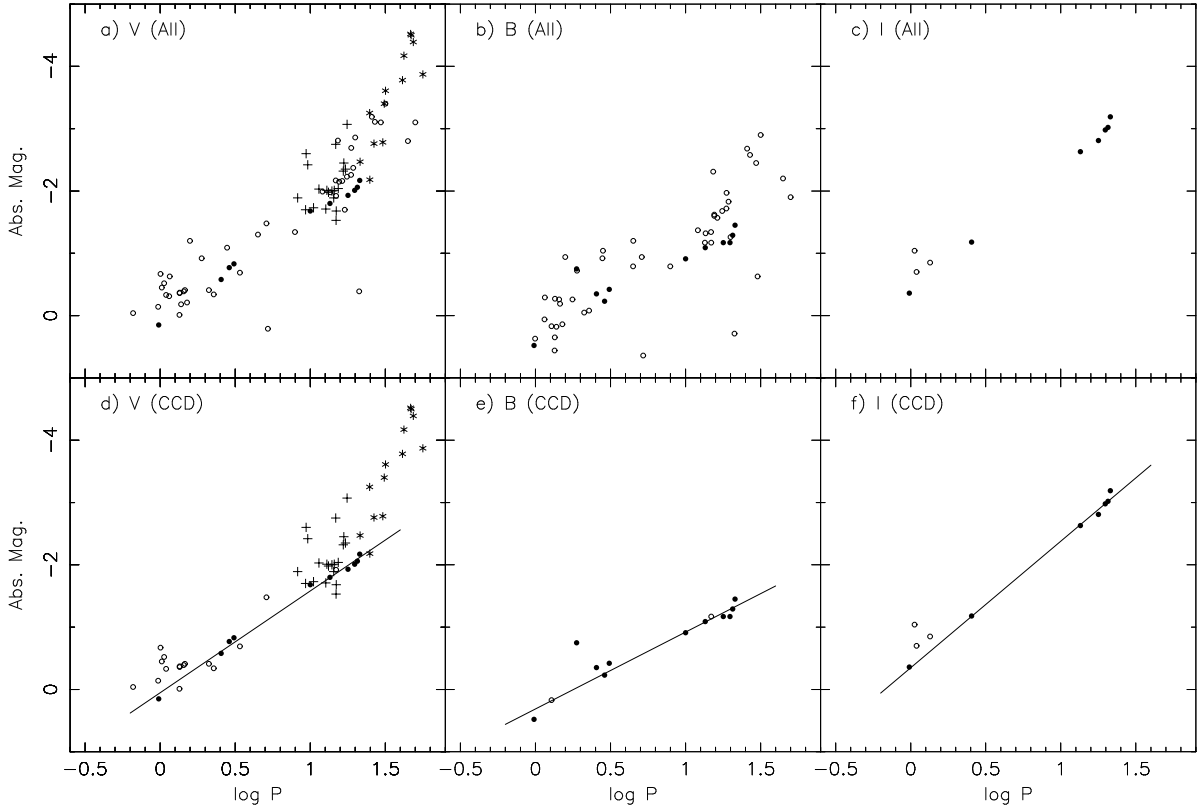


FIG. 9.— Period-luminosity plots for Population II Cepheids. In the top row (a, b, c) we include all the data available for Population II Cepheids in Galactic GCs (NGC 6388 and NGC 6441: filled circles; all others: open circles) and the Large Magellanic Cloud (W Virginis stars: pluses; RV Tauri: asterisks). The bottom row (d, e, f) shows only those stars with CCD photometry. We also include in these figures the period-luminosity lines found for the NGC 6388 and NGC 6441 Population II Cepheids.

## 5. SUMMARY AND CONCLUSIONS

We have found 57 variable stars in the inner regions of NGC 6441 using the HST snapshot observing program, 41 of which were previously undiscovered. Of the RRL stars found in this survey, 26 are RRab stars and 12 are RRc stars. There are no clear differences in the properties of the RRL stars in the inner and outer regions of the cluster. This is illustrated in the period-amplitude diagram where the RRL stars in this survey are located in the same regions as those found in the

ground-based surveys (Layden et al. 1999; Pritzl et al. 2001). Combining the RRL stars in this survey and those found in ground-based surveys, we find the mean periods of the RRab and RRc stars to be 0.759 d and 0.375 d. This reaffirms that NGC 6441 is unusual when compared to other Galactic GCs in that, whereas it is a metal-rich GC, its RRL stars have mean periods that are similar to, if not greater than, those of very metal-poor GCs. This reconfirms the conclusions of Pritzl et al. (2001) that the RRL stars in NGC 6441 are unusually bright for their metallicity. This breaks the general metallicity-luminosity

relation for the RRL stars and has consequences on their use as distance indicators. A possible trend of the inner RRab stars ( $r < 20$  arcsec) having a longer mean period than the remaining RRab stars was also detected, but further observations will be needed to make definitive conclusions. We also used the  $I$ -band photometry to derive P-L relations for the RRL stars.

We also found six P2Cs in NGC 6441 making it, along with its "sister" cluster NGC 6388, the most metal-rich GC to contain this type of variable star. Five of the P2Cs are of W Vir type and one is a BL Her star. Also, V118 may be an additional BL Her variable given its bright magnitude and long period compared to the RRL stars. Under the assumption that the RRL stars in NGC 6388 and NGC 6441 have absolute magnitudes similar to those of metal-poor GCs, we have derived the  $B$ ,  $V$ , and  $I$  period-luminosity relations for their P2Cs. These P-L relations do not show the change in slope around  $P = 10$  day

which some have suggested and show a surprisingly tight correlation. We also find that only one P-L relation is needed to describe the data, i.e., it appears that the P2Cs are pulsating in one mode. An examination of the P2Cs in GCs for which  $V$  CCD photometry is available indicates that the break in the slope of the P2C P-L relation does not come at periods of 10 or 12 days, but at longer periods, where the P2Cs begin to take on RV Tau characteristics.

Support for Proposal number SNAP 8251 was provided by NASA through a grant from the Space Telescope Science Institute, which is operated by the Association of Universities for Research in Astronomy, Incorporated, under NASA contract NAS5-26555.

Support for M.C. was provided by Proyecto de Inicio DIPUC 2002-04E and Proyecto FONDECYT Regular 1030954.

## REFERENCES

- Alard, C. 2000, *A&AS*, 144, 363  
 Alcock, C., et al. 1998, *AJ*, 115, 1921  
 Arp, H. C. 1955a, *AJ*, 60, 1  
 Arp, H. C. 1955b, *AJ*, 60, 317  
 Barnes, S. A. 1968, *AJ*, 73, 579  
 Benedict, G. F., et al. 2002, *AJ*, 123, 473  
 Blanco, B. M. 1992, *AJ*, 103, 1872  
 Bono, G., Caputo, F., Castellani, V., Marconi, M., & Storm, J. 2001, *MNRAS*, 326, 1183  
 Bono, G., Caputo, F., Castellani, V., & Marconi, M. 1997a, *A&AS*, 121, 327  
 Bono, G., Caputo, F., & Santolamazza, P. 1997b, *A&A*, 317, 171  
 Borissova, J., Catelan, M., & Valchev, T. 2001, *MNRAS*, 324, 77  
 Borissova, J., Ivanov, V. D., & Catelan, M. 2000, *IBVS*, 4919, 1  
 Butler, R. F., et al. 1998, *MNRAS*, 296, 379  
 Castellani, V. 1983, *MmSAIt*, 54, 141  
 Catelan, M., Sweigart, A. V., & Borissova, J. 1998, in *ASP Conf. Ser. 135, A Half Century of Stellar Pulsation Interpretation: A Tribute to Arthur N. Cox*, ed. P. A. Bradley & J. A. Guzik (San Francisco: ASP), 41  
 Clement, C. M. 2000, in *ASP Conf. Ser. 203, The Impact of Large-Scale Surveys on Pulsating Star Research*, ed. L. Szabados & D. W. Kurtz (IAU Colloq. 176) (San Francisco: ASP), 266  
 Clement, C. M., & Hazen, M. L. 1989, *AJ*, 97, 414  
 Clement, C. M., & Hogg, H. S. 1978, *AJ*, 83, 167  
 Clement, C. M., Hogg, H. S., & Wells, T. R. 1980, *AJ*, 85, 1604  
 Clement, C. M., Hogg, H. S., & Wells, T. R. 1985, *AJ*, 90, 1238  
 Clement, C. M., Hogg, H. S., Yee, A. 1988, *AJ*, 96, 1642  
 Clement, C. M., Ip, P., & Robert, N. 1984, *AJ*, 89, 1707  
 Demers, S. 1969, *AJ*, 74, 925  
 Demers, S. 1971, *AJ*, 76, 445  
 Demers, S., & Harris, W. E. 1974, *AJ*, 79, 627  
 Demers, S., & Wehlau, A. 1971, *AJ*, 76, 916  
 Dickens, R. J., & Carey, J. V. 1967, *Roy. Obs. Bull. no. 129*, 335  
 Freedman, W. L., et al. 2001, *ApJ*, 553, 47  
 Fusi Pecci, F., & Bellazzini, M. 1997, in *The Third Conference on Faint Blue Stars*, ed. A. G. Davis Philip, J. W. Liebert, & R. A. Saffer (Schenectady: L. Davis Press), 255  
 Fusi Pecci, F., Bellazzini, M., & Ferraro, F. R. 1996, in *ASP Conf. Ser. 92, Formation of the Galactic Halo... Inside and Out*, eds. H. Morrison & A. Sarajedini (San Francisco: ASP), 221  
 Gingold, R. A. 1985, *MmSAIt*, 56, 169  
 Harris, H. C. 1985, in *Cepheids: Theory and Observations*, IAU Colloquium No. 82, ed. B. F. Madore (Cambridge: Cambridge Univ. Press), 232  
 Harris, W. E. 1996, *AJ*, 112, 1487  
 Harris, W. E., et al. 1997, *AJ*, 114, 1030  
 Holtzman, J. A., Burrows, C. J., Casertano, S., Hester, J. J., Tauger, J. T., Watson, A. M., & Worthey, G. 1995, *PASP*, 107, 1065  
 Kaluzny, J., & Krzeminski, W. 1993, *MNRAS*, 264, 785  
 Kaluzny, J., Kubiak, M., Szymanski, M., Udalski, A., Krzeminski, W., & Mateo, M. 1997, *A&AS*, 125, 343  
 Kinman, T. D. 1959, *MNRAS*, 119, 538  
 Kopacki, G. 2001, *A&A*, 369, 862  
 Kopacki, G., Kołaczowski, Z., & Pigulski, A. 2003, *A&A*, 398, 541  
 Kwee, K. K. 1968, *Bull. Astr. Inst. Netherlands*, 19, 374  
 Layden, A. C., Ritter, L. A., Welch, D. L., & Webb, T. M. A. 1999, *AJ*, 117, 1313  
 Layden, A. C., & Sarajedini, A. 2000, *AJ*, 119, 1760  
 Layden, A. C., & Sarajedini, A. 2003, *AJ*, 125, 208  
 Lee, S. W. 1974, *Observatory*, 94, 74  
 Lee, Y.-W., Demarque, P., & Zinn, R. 1990, *ApJ*, 350, 155  
 Lee, Y.-W., Demarque, P., & Zinn, R. 1994, *ApJ*, 423, 248  
 Lee, Y.-W., & Zinn, R. 1990, in *ASP Conf. Ser. 11, Confrontation Between Stellar Pulsation and Evolution*, ed. C. Cacciari & G. Clementini (San Francisco: ASP), 26  
 Longmore, A. J., Dixon, R., Skillen, I., Jameson, R. F., & Fernley, J. A. 1990, *MNRAS*, 247, 684  
 McNamara, D. H. 1995, *AJ*, 109, 2134  
 Moehler, S., Sweigart, A. V., & Catelan, M. 1999, *A&A*, 351, 519  
 Nemeč, J. M., Nemeč, A. F. L., & Lutz, T. E. 1994, *AJ*, 108, 222  
 Oosterhoff, P. Th. 1938, *Observatory*, 62, 104  
 Pike, C. D., & Meston, C. J. 1977, *MNRAS*, 180, 613  
 Pinto, G., & Rosino, L. 1977, *A&AS*, 28, 427  
 Piotto, G., et al. 1997, in *Advances in Stellar Evolution*, ed. R. T. Rood & A. Renzini (Cambridge: Cambridge Univ. Press), 84  
 Pritzl, B., Smith, H. A., Catelan, M., & Sweigart, A. V. 2000, *ApJ*, 530, L41  
 Pritzl, B., Smith, H. A., Catelan, M., & Sweigart, A. V. 2001, *AJ*, 122, 2600  
 Pritzl, B., Smith, H. A., Catelan, M., & Sweigart, A. V. 2002, *AJ*, 124, 949  
 Raimondo, G., Castellani, V., Cassisi, S., Brocato, E., & Piotto, G. 2002, *ApJ*, 569, 975  
 Ree, C. H., Yoon, S.-J., Rey, S.-C., & Lee, Y.-W. 2002, in *ASP Conf. Ser. 265, Omega Centauri: A Unique Window Into Astrophysics*, ed. F. van Leeuwen, G. Piotto, & J. Hughes (San Francisco: ASP), 101  
 Renzini, A. 1983, *MmSAIt*, 54, 335  
 Rich, R. M., et al. 1997, *ApJ*, 484, L25  
 Russeva, T., Ilieva, L., & Russev, R. 1982, *IBVS*, 2223, 1  
 Russeva, T., & Russev, R. 1979, *Peremennye Zvezdy*, 21, 169  
 Russeva, T., & Russev, R. 1983, *Peremennye Zvezdy*, 22, 49  
 Sandage, A., & Wildey, R. 1967, *ApJ*, 150, 469  
 Searle, L., & Zinn, R. 1978, *ApJ*, 225, 357  
 Silbermann, N. A., & Smith, H. A. 1995, *AJ*, 110, 704  
 Silbermann, N. A., Smith, H. A., Bolte, M., & Hazen, M. L. 1994, *AJ*, 107, 1764  
 Smith, H. A., & Wehlau, A. 1985, *ApJ*, 298, 572  
 Stetson, P. B. 1987, *PASP*, 99, 191  
 Stetson, P. B. 1994, *PASP*, 106, 250  
 Stetson, P. B. 1996, *PASP*, 108, 851  
 Stetson, P. B. 1998, *PASP*, 110, 1448  
 Stetson, P. B., et al. 1998, *ApJ*, 508, 491  
 Stetson, P. B., et al. 1999, *AJ*, 117, 247  
 Strader, J., Everitt, H. O., & Danford, S. 2002, *MNRAS*, 335, 621  
 Sweigart, A. V. 2002, in *Highlights of Astronomy*, ed. H. Rickman (San Francisco: ASP), 12, 292  
 Sweigart, A. V., & Catelan, M. 1998, *ApJ*, 501, L63  
 van den Bergh, S. 1967, *PASP*, 79, 460  
 Walker, A. R. 2000, in *ASP Conf. Ser. 203, The Impact of Large-Scale Surveys on Pulsating Star Research*, ed. L. Szabados & D. W. Kurtz (San Francisco: ASP), 165  
 Wallerstein, G. 1970, *ApJ*, 160, 345  
 Wallerstein, G. 2002, *PASP*, 114, 689  
 Wehlau, A., & Bohlender, D. 1982, *AJ*, 87, 780  
 Wehlau, A., & Butterworth, S. 1990, *AJ*, 100, 686  
 Wehlau, A., & Froelich, N. 1994, *AJ*, 108, 134  
 Wehlau, A., & Hogg, H. S. 1978, *AJ*, 83, 946  
 Wehlau, A., & Hogg, H. S. 1984, *AJ*, 89, 1005  
 Wehlau, A., & Hogg, H. S. 1985, *AJ*, 90, 2514  
 Wehlau, A., Hogg, H. S., & Butterworth, S. 1990, *AJ*, 99, 1159  
 Welch, D. L., & Stetson, P. B. 1993, *AJ*, 105, 1813  
 Zinn, R. 1980, *ApJS*, 42, 19

TABLE 1  
NGC 6441 HST OBSERVATION LOG

HST Dataset Name	Date	Filter	Exposure Times (sec)
U2HJ0103T	1994 August 08	F439W	50
U2HJ0104T	1994 August 08	F439W	500
U2VO0801T	1995 September 12	F555W	14
U2VO0802T	1995 September 12	F555W	50
U2VO0803T	1995 September 12	F439W	50
U2VO0804T	1995 September 12	F439W	160
U2VO0805T	1995 September 12	F439W	160
U39U010ET	1996 August 8	F547M	80
U39U010FT	1996 August 8	F547M	80
U39U010GT	1996 August 8	F547M	20
U39U010HT	1996 August 8	F547M	20
U59V1101R	1999 March 16	F439W	50
U59V1102R	1999 March 16	F555W	10
U59V1103R	1999 March 16	F814W	10
U59V1201R	1999 April 6	F439W	50
U59V1202R	1999 April 6	F555W	10
U59V1203R	1999 April 6	F814W	10
U59V0501R	1999 April 18	F439W	50
U59V0502R	1999 April 18	F555W	10
U59V0503R	1999 April 18	F814W	10
U59V0301R	1999 July 15	F439W	80
U59V0302R	1999 July 15	F555W	10
U59V0303R	1999 July 15	F814W	10
U59V0101R	1999 July 25	F439W	80
U59V0102R	1999 July 25	F555W	10
U59V0103R	1999 July 25	F814W	10
U59V2001R	2000 August 19	F439W	80
U59V2002R	2000 August 19	F555W	10
U59V2003R	2000 August 19	F814W	10
U59V0701R	1999 August 21	F439W	80
U59V0702R	1999 August 21	F555W	10
U59V0703R	1999 August 21	F814W	10
U59V0901R	1999 August 23	F439W	80
U59V0902R	1999 August 23	F555W	10
U59V0903R	1999 August 23	F814W	10
U59V0401R	1999 September 2	F439W	80
U59V0402R	1999 September 2	F555W	10
U59V0403R	1999 September 2	F814W	10
U59V1001R	1999 September 4	F439W	80
U59V1002R	1999 September 4	F555W	10
U59V1003R	1999 September 4	F814W	10
U59V1601R	1999 September 16	F439W	80
U59V1602R	1999 September 16	F555W	10
U59V1603R	1999 September 16	F814W	10
U59V0601R	1999 September 19	F439W	80
U59V0602R	1999 September 19	F555W	10
U59V0603R	1999 September 19	F814W	10
U59V1901R	1999 September 19	F439W	80
U59V1902R	1999 September 19	F555W	10
U59V1903R	1999 September 19	F814W	10
U59V0201R	2000 February 29	F439W	80
U59V0202R	2000 February 29	F555W	10

TABLE 1—*Continued*

HST Dataset Name	Date	Filter	Exposure Times (sec)
U59V0203R	2000 February 29	F814W	10
U59V1401R	2000 March 4	F439W	80
U59V1402R	2000 March 4	F555W	10
U59V1403R	2000 March 4	F814W	10
U59V1701R	2000 May 23	F439W	80
U59V1702R	2000 May 23	F555W	10
U59V1703R	2000 May 23	F814W	10
U59V1301R	2000 May 26	F439W	80
U59V1302R	2000 May 26	F555W	10
U59V1303R	2000 May 26	F814W	10
U59V0801R	2000 June 30	F439W	80
U59V0802R	2000 June 30	F555W	10
U59V0803R	2000 June 30	F814W	10

TABLE 2  
NGC 6441 *B* PHOTOMETRY OF VARIABLE STARS

ID	HJD	<i>B</i>	$\sigma_B$
V001	51374.930	20.830	0.078
V001	51410.434	20.476	0.145
V001	51411.773	20.376	0.111
V001	51413.652	20.225	0.102
V001	51424.422	19.308	0.075
V001	51425.836	19.194	0.069
V001	51437.648	18.445	0.067
V001	51440.871	18.418	0.100
V001	51440.949	18.347	0.044
V006	49972.754	16.118	0.052
V006	49972.754	16.118	0.052
V006	49972.754	16.123	0.046
V006	49972.754	16.123	0.046
V006	49972.758	16.120	0.041
V006	51374.930	16.974	0.108
V006	51385.414	15.449	0.139
V006	51410.434	15.640	0.038
V006	51411.773	15.791	0.025
V006	51413.652	16.036	0.041
V006	51424.422	16.173	0.130
V006	51425.836	15.774	0.112
V006	51440.871	17.316	0.042
V006	51440.949	17.340	0.099

Note. — The complete version of this table is in the electronic edition of the Journal. The printed edition contains only a sample.

TABLE 3  
NGC 6441 V PHOTOMETRY OF VARIABLE STARS

ID	HJD	$V$	$\sigma_V$
V001	51374.934	18.945	0.072
V001	51385.418	19.091	0.059
V001	51411.777	18.589	0.092
V001	51413.656	18.451	0.095
V001	51424.422	17.588	0.046
V001	51425.836	17.471	0.050
V001	51437.648	16.847	0.023
V001	51440.871	16.765	0.079
V001	51440.949	16.702	0.084
V006	49972.746	14.681	0.056
V006	49972.750	14.744	0.084
V006	51374.934	15.470	0.049
V006	51385.418	14.311	0.086
V006	51410.434	14.701	0.310
V006	51411.777	14.659	0.073
V006	51413.656	14.864	0.065
V006	51424.422	15.061	0.080
V006	51425.836	14.817	0.067
V006	51440.871	15.557	0.043
V006	51440.949	15.580	0.042
V006	51725.844	14.497	0.060

Note. — The complete version of this table is in the electronic edition of the Journal. The printed edition contains only a sample.

TABLE 4  
 NGC 6441 *I* PHOTOMETRY OF VARIABLE STARS

ID	HJD	<i>I</i>	$\sigma_I$
V001	51374.934	13.340	0.045
V001	51385.422	13.503	0.042
V001	51410.438	13.366	0.064
V001	51411.777	13.248	0.077
V001	51413.656	13.224	0.074
V001	51424.426	12.800	0.056
V001	51425.840	12.761	0.057
V001	51437.652	12.918	0.108
V001	51440.875	12.687	0.091
V001	51440.953	12.654	0.074
V006	51374.934	13.786	0.029
V006	51385.422	12.876	0.065
V006	51410.438	12.863	0.058
V006	51411.777	12.897	0.045
V006	51413.656	13.081	0.035
V006	51424.426	13.577	0.041
V006	51425.840	13.375	0.066
V006	51440.875	13.761	0.019
V006	51440.953	13.758	0.031

Note. — The complete version of this table is in the electronic edition of the Journal. The printed edition contains only a sample.

TABLE 5  
NGC 6441 VARIABLE STAR MEAN PROPERTIES

ID	RA	Dec	Period (d)	$\langle B \rangle$	$A_B$	$\langle V \rangle$	$A_V$	$\langle I \rangle$	$A_I$	Classification
001	17:50:17.13	-37:03:50.3	89.9:	19.853	2.691	17.848	2.633	13.092	0.924	LPV
006	17:50:15.65	-37:02:16.3	21.365	16.117	2.017	14.885	1.274	13.231	1.125	P2C
010	17:50:19.54	-37:04:05.0	155:	18.958	1.897	16.618	1.817	12.843	1.079	LPV
017	17:50:07.36	-37:02:40.7	257.6	18.712	0.985	16.802	0.938	13.648	0.285	LPV
040	17:50:10.54	-37:04:00.6	0.64800	18.397	1.331	17.572	1.103	16.541	0.727	RRab
055	17:50:12.46	-37:02:28.2	0.69750	18.333	1.507	17.562	1.054	16.416	0.722	RRab
056	17:50:11.13	-37:02:39.9	0.90582	18.239	1.034	17.410	0.776	16.253	0.573	RRab
057	17:50:10.44	-37:02:56.1	0.69438	18.325	1.524	17.575	1.046	16.435	0.808	RRab
058	17:50:14.72	-37:03:07.2	0.68538	18.363	1.307	17.581	0.846	16.361	0.648	RRab
063	17:50:11.34	-37:02:47.4	0.69781	18.379	1.242	17.572	0.881	16.431	0.481	RRab
064	17:50:09.64	-37:03:07.7	0.71710	18.366	1.359	17.592	0.967	16.399	0.720	RRab
065	17:50:13.20	-37:02:30.2	0.75850	18.528	0.999	17.688	0.772	16.479	0.362	RRab
075	17:50:12.50	-37:03:40.6	0.40502	18.139	0.469	17.471	0.355	16.498	0.219	RRc
093	17:50:06.34	-37:02:45.1	0.34004	18.020	0.592	17.474	0.412	16.670	0.165	RRc
095	17:50:08.51	-37:04:13.8	0.089928	18.369	0.793	17.605	0.559	16.604	0.356	$\delta$ Scuti
102	17:50:09.63	-37:04:11.1	0.30889	18.139	0.763	17.526	0.486	16.657	0.319	RRc
105	17:50:12.32	-37:02:52.6	111.6	18.137	1.266	16.151	1.487	13.039	0.867	LPV; SV7
106	17:50:10.61	-37:03:26.0	0.36092	18.304	0.673	17.650	0.426	16.670	0.287	RRc; SV14
107	17:50:15.24	-37:03:07.1	0.73891	18.499	1.076	17.650	0.853	16.443	0.655	RRab
108	17:50:14.45	-37:02:42.9	0.34419	18.188	0.589	17.531	0.426	16.596	0.257	RRc
109	17:50:14.72	-37:02:50.0	0.36455	18.285	0.606	17.611	0.470	16.633	0.299	RRc
110	17:50:14.07	-37:03:00.8	0.76867	18.198	1.359	17.399	0.878	16.317	0.523	RRab
111	17:50:13.69	-37:02:57.8	0.74464	18.386	1.154	17.552	0.781	16.305	0.345	RRab
112	17:50:13.61	-37:02:54.3	0.61419	18.177	1.542	17.363	1.067	16.245	0.652	RRab
113	17:50:13.56	-37:02:56.6	0.58845	18.335	1.618	17.605	1.136	16.589	0.844	RRab
114	17:50:13.46	-37:02:53.3	0.67389	18.366	1.342	17.610	1.015	16.485	0.622	RRab
115	17:50:13.27	-37:02:46.4	0.86311	18.458	0.722	17.552	0.536	16.291	0.444	RRab
116	17:50:13.12	-37:03:22.7	0.58229	18.264	1.713	17.612	1.257	16.544	0.790	RRab
117	17:50:13.10	-37:03:12.2	0.74529	18.314	1.451	17.557	0.908	16.456	0.576	RRab
118	17:50:12.50	-37:03:20.8	0.97923	18.048	1.337	17.201	0.846	16.061	0.568	RRab?;P2C?
119	17:50:12.45	-37:03:01.3	0.68628	18.203	1.525	17.511	1.014	16.422	0.613	RRab
120	17:50:12.19	-37:02:53.5	0.36396	18.224	0.586	17.558	0.430	16.600	0.271	RRc
121	17:50:12.18	-37:02:59.5	0.83748	18.428	0.715	17.522	0.637	16.381	0.360	RRab
122	17:50:11.78	-37:03:04.8	0.74270	18.341	1.141	17.531	0.838	16.392	0.516	RRab
123	17:50:11.44	-37:03:06.9	0.33566	18.212	0.655	17.532	0.507	16.612	0.334	RRc
124	17:50:09.73	-37:02:46.9	0.31588	18.273	0.667	17.631	0.459	16.717	0.370	RRc
125	17:50:14.36	-37:02:44.7	0.33679	18.258	0.681	17.569	0.502	16.659	0.357	RRc
126	17:50:12.54	-37:03:12.0	20.625	16.282	1.771	14.997	1.110	13.402	0.923	P2C
127	17:50:12.08	-37:03:12.3	19.773	16.398	1.521	15.048	1.057	13.441	0.869	P2C
128	17:50:11.80	-37:02:59.1	13.519	16.475	0.659	15.257	0.500	13.795	0.370	P2C
129	17:50:12.87	-37:03:18.1	17.832	16.395	1.317	15.128	0.918	13.610	0.774	P2C
130	17:50:14.43	-37:03:04.8	48.90	17.412	0.799	15.500	0.628	13.364	0.406	LPV
131	17:50:15.52	-37:03:07.4	122.8	17.848	1.841	15.914	1.667	12.959	1.012	LPV
132	17:50:12.87	-37:03:08.6	2.54737	17.218	1.623	16.478	0.900	15.241	0.784	P2C
133	17:50:13.98	-37:02:57.0	122.9	18.401	0.462	16.371	0.520	12.973	0.129	LPV
134	17:50:15.37	-37:03:19.5	128.9	18.655	0.869	16.731	1.088	12.980	0.556	LPV
135	17:50:12.61	-37:02:38.0	162.6	18.295	4.074	16.574	3.919	13.777	2.786	LPV
136	17:50:12.69	-37:03:16.2	0.80573	18.235	0.854	17.360	0.580	16.158	0.273	RRab
137	17:50:11.85	-37:03:03.0	51.2	18.524	0.446	16.792	0.593	13.148	0.296	LPV
138	17:50:14.00	-37:03:07.7	0.80199	18.603	0.660	17.707	0.424	16.520	0.181	RRab
139	17:50:13.58	-37:03:16.2	249.1	17.792	8.083	16.009	5.819	12.982	1.716	LPV
140	17:50:10.80	-37:03:05.9	0.35181	18.244	0.421	17.539	0.372	16.643	0.277	RRc; SV15
141	17:50:13.98	-37:03:16.2	0.84475	18.417	0.451	17.536	0.404	16.329	0.296	RRab
142	17:50:13.83	-37:02:49.7	0.88400	18.422	0.407	17.523	0.349	16.262	0.194	RRab
143	17:50:13.75	-37:02:47.8	0.86279	18.425	0.664	17.532	0.487	16.305	0.284	RRab
144	17:50:11.34	-37:02:59.6	70.6:	18.017	0.485	16.103	0.377	13.074	0.130	LPV
145	17:50:12.72	-37:03:09.6	0.55581	18.064	0.505	17.372	0.355	16.248	0.252	RRc



TABLE 6  
COMPARISON OF NGC 6441 VARIABLE STARS IN THE HST AND GROUND-BASED SURVEYS

ID	$\langle V \rangle_{\text{HST}}$	$A_{V,\text{HST}}$	$\langle B \rangle_{\text{HST}}$	$A_{B,\text{HST}}$	$\langle V \rangle_{\text{GB}}$	$A_{V,\text{GB}}$	$\langle B \rangle_{\text{GB}}$	$A_{B,\text{GB}}$
40	17.572	1.103	18.397	1.331	17.512	1.08	18.242	1.45
55	17.562	1.054	18.333	1.507	17.523	0.97	18.194	1.25
56	17.410	0.776	18.191	1.159	16.497	...	17.595	0.64
57	17.575	1.046	18.325	1.524	17.313	0.95	18.161	1.25
58	17.581	0.846	18.363	1.307	16.868	...	17.705	0.70
63	17.572	0.881	18.379	1.242	17.064	...	17.802	0.78
64	17.592	0.967	18.366	1.359	16.986	...	18.274	0.95
65	17.688	0.772	18.528	0.999	16.911	0.40	17.989	0.61
75	17.471	0.355	18.139	0.469	17.349	...	18.027	0.46
93	17.474	0.412	18.020	0.592	17.332	0.54	18.057	...
95	17.605	0.559	18.369	0.793	17.611	0.55	18.256	0.67
102	17.526	0.486	18.139	0.763	15.834	...	17.257	0.32

TABLE 7  
NGC 6441 & NGC 6388 POPULATION II CEPHEID MEAN PROPERTIES

Cluster	ID	Period (d)	$\log P$	$\langle V \rangle$	$\langle B \rangle$	$\langle I \rangle$	$M_V$	$M_B$	$M_I$
NGC 6388	18	2.89	0.4609	15.62	16.56	...	-0.77	-0.23	...
NGC 6388	29	1.88	0.2742	...	16.04	...	...	-0.75	...
NGC 6388	36	3.10	0.4914	15.56	16.37	...	-0.83	-0.42	...
NGC 6388	37	10.0	1.0000	14.71	15.88	...	-1.68	-0.91	...
NGC 6441	6	21.365	1.3297	14.89	16.12	13.23	-2.16	-1.44	-3.18
NGC 6441	118	0.97923	-0.0091	17.20	18.05	16.06	0.15	0.49	-0.35
NGC 6441	126	20.625	1.3144	15.00	16.28	13.40	-2.05	-1.28	-3.01
NGC 6441	127	19.773	1.2961	15.05	16.40	13.44	-2.00	-1.16	-2.97
NGC 6441	128	13.519	1.1309	15.26	16.48	13.80	-1.79	-1.08	-2.62
NGC 6441	129	17.832	1.2512	15.13	16.40	13.61	-1.92	-1.16	-2.80
NGC 6441	132	2.54737	0.4061	16.48	17.22	15.24	-0.57	-0.34	-1.17

TABLE 8  
GALACTIC GLOBULAR CLUSTER POPULATION II CEPHEID MEAN PROPERTIES

Cluster	ID	Period (d)	$\log P$	$\langle V \rangle$	$\langle B \rangle$	$\langle I \rangle$	$M_V$	$M_B$	$M_I$	References	
NGC 2419	18	1.578524	0.1983	18.8	19.16	...	-1.2	-0.94	...	PR77	
NGC 2808	10	1.76528	0.2468	...	15.56	...	...	-0.26	...	CH89	
Palomar 3	4	3.402	0.532	19.28	...	...	-0.69	...	...	BIC00	
NGC 4372	24	3.13	0.50	17.04	18.22	15.75	2.00	2.79	1.20	KK93	
	28	2.60	0.41	17.40	18.97	15.49	2.36	3.54	0.94		
$\omega$ Cen	52	0.6604	-0.1802	13.95	...	...	-0.04	...	...	K97	
	60	1.3496	0.1302	13.63	...	...	-0.36	...	...		
	61	2.2743	0.3568	13.65	...	...	-0.34	...	...		
	92	1.3461	0.1291	13.98	...	...	-0.01	...	...		
	O123	1.0253	0.0109	13.54	...	...	-0.45	...	...		
	O156	1.0066	0.0029	13.32	...	...	-0.67	...	...		
	O161	0.9707	-0.0129	13.85	...	...	-0.14	...	...		
	92	1.345	0.129	13.92	14.49	...	-0.07	0.38	...		K68
	1	29.18	1.47	10.89	11.66	...	-3.10	-2.45	...		DC67
	29	14.73	1.17	11.82	12.77	...	-2.17	-1.34	...		
	43	1.1568	0.0633	13.36	13.82	...	-0.63	-0.29	...		
	48	4.474	0.651	12.69	13.32	...	-1.30	-0.79	...		
60	1.34946	0.1302	13.45	13.84	...	-0.54	-0.27	...			
61	2.27351	0.3567	13.40	14.03	...	-0.59	-0.08	...			
92	1.34577	0.1290	13.93	14.46	...	-0.06	0.35	...			
M3	154	15.285	1.184	12.32	12.83	...	-2.81	-2.31	...	DC67	
	S7	1.3270	0.1229	...	...	...	...	...	...	SED02	
M5	42	25.728	1.410	11.28	11.82	...	-3.19	-2.68	...	K68	
	84	26.62	1.43	11.36	11.92	...	-3.11	-2.58	...		
	42	25.7325	1.4105	11.31	11.85	...	-3.16	-2.65	...	DC67	
	84	26.4945	1.4232	11.36	11.94	...	-3.11	-2.56	...		
M80	1	16.3042	1.2123	13.42	14.19	...	-2.16	-1.57	...	WHB90	
M13	1	1.459033	0.1641	14.086	...	...	-0.41	...	...	KKP03	
	2	5.110818	0.7085	13.012	...	...	-1.48	...	...		
	6	2.112918	0.3249	14.078	...	...	-0.41	...	...		
	1	1.459033	0.1641	14.07	14.32	...	-0.42	-0.19	...	RR83	
	2	5.110818	0.7085	13.12	13.57	...	-1.37	-0.94	...		
	6	2.112918	0.3249	14.03	14.46	...	-0.46	-0.05	...		
	32	21.165	1.326	14.10	14.80	...	-0.39	0.29	...	RIR82	
	12	5.21753	0.7175	14.70	15.15	...	0.21	0.64	...	RR79	
	1	1.459252	0.1641	14.19	14.45	...	-0.30	-0.06	...	PM77	
	2	5.110939	0.7085	13.10	13.52	...	-1.39	-0.99	...		
	6	2.112867	0.3249	14.11	14.54	...	-0.38	0.03	...		
	1	1.458997	0.1641	14.00	14.20	...	-0.49	-0.31	...	D71	
	2	5.110939	0.7085	12.98	13.29	...	-1.51	-1.22	...		
	6	2.112867	0.3249	14.00	14.42	...	-0.49	-0.09	...		
	1	1.458981	0.1640	13.69	14.19	...	-0.80	-0.32	...	DC67	
	2	5.11128	0.7085	13.85	14.45	...	-0.64	-0.06	...		

TABLE 8—Continued

Cluster	ID	Period (d)	$\log P$	$\langle V \rangle$	$\langle B \rangle$	$\langle I \rangle$	$M_V$	$M_B$	$M_I$	References
	6	2.112897	0.3249	12.78	13.34	...	-1.71	-1.17	...	
M12	1	15.527	1.191	...	12.60	...	...	-1.62	...	CHY88
NGC 6229	8	14.840457	1.1714	15.53	16.29	...	-1.92	-1.17	...	BCV01
	22	15.8373	1.1997	...	...	...	...	...	...	
M10	2	18.7226	1.2724	...	...	...	...	...	...	CHW85
	3	7.831	0.894	...	...	...	...	...	...	
	2	18.728	1.272	11.83	12.65	...	-2.26	-1.72	...	K68
	3	7.908	0.898	12.75	13.58	...	-1.34	-0.79	...	
	2	18.7351	1.2727	13.16	13.90	...	-0.93	-0.47	...	DC67
	3	7.87	0.90	14.09	14.89	...	0.00	0.52	...	
M19	1	16.92	1.23	...	...	...	...	...	...	CH78
	2	14.139	1.150	...	...	...	...	...	...	
	3	16.5	1.2	...	...	...	...	...	...	
	4	2.4326	0.3861	...	...	...	...	...	...	
NGC 6284	1	4.48121	0.6514	...	15.88	...	...	-1.20	...	CHW80
	4	2.81873	0.4501	...	16.04	...	...	-1.04	...	
M92	7	1.0614007	0.0259	14.15	...	13.61	-0.52	...	-1.04	K01
M9	12	1.340204	0.1271	...	16.62	...	...	0.56	...	CIR84
M14	1	18.729	1.273	14.03	15.35	...	-2.69	-1.97	...	WF94
	2	2.794708	0.4463	15.63	16.40	...	-1.09	-0.92	...	
	7	13.6038	1.1337	14.74	16.00	...	-1.98	-1.32	...	
	17	12.091	1.082	14.73	15.95	...	-1.99	-1.37	...	
	76	1.890265	0.2765	15.80	16.60	...	-0.92	-0.72	...	
	1	18.734	1.273	14.06	15.28	...	-2.66	-2.04	...	DW71
	2	2.794708	0.4463	15.65	16.39	...	-1.07	-0.93	...	
	7	13.603	1.134	14.80	16.02	...	-1.92	-1.30	...	
	17	12.085	1.082	14.81	15.95	...	-1.91	-1.37	...	
	76	1.89003	0.2765	15.84	16.60	...	-0.88	-0.72	...	
M28	4	13.462	1.129	...	14.21	...	...	-1.17	...	WB90
	17	45.9	1.7	11.9:	13.5:	...	-3.1:	-1.9:	...	
	4	13.458	1.129	...	14.25	...	...	-1.13	...	WH84
	17	46.1	1.7	...	13.5	...	...	-1.9	...	
	21	29.93	1.48	...	14.75	...	...	-0.63	...	
	22	0.99538	-0.0020	...	15.75	...	...	0.37	...	
M22	11	1.69050	0.2280	...	...	...	...	...	...	WH78
M54	1	1.34769	0.1296	17.257	...	16.589	-0.368	...	-0.849	LS00
	2	1.09461	0.0393	17.292	...	16.738	-0.333	...	-0.700	
NGC 6752	1	1.3782	0.1393	12.97	13.37	...	-0.18	0.18	...	L74
M56	1	1.510019	0.1790	15.46	16.01	...	-0.21	0.14	...	WH85
	6	45.00	1.65	12.9:	13.7:	...	-2.8:	-2.2:	...	
M15	142	1.280	0.107	...	15.66	...	...	0.17	...	B98
	1	1.437712	0.1577	14.996	...	...	-0.394	...	...	SS95
	1	1.44	0.16	14.89	15.23	...	-0.50	-0.26	...	H85
	72	1.14	0.06	15.08	15.55	...	-0.31	0.06	...	
	86	17.11	1.23	13.7:	...	...	-1.7:	...	...	
	1	1.437395	0.1576	14.89	15.23	...	-0.50	-0.26	...	DC67

TABLE 8—*Continued*

Cluster	ID	Period (d)	$\log P$	$\langle V \rangle$	$\langle B \rangle$	$\langle I \rangle$	$M_V$	$M_B$	$M_I$	References
M2	1	15.5647	1.1921	13.36	13.97	...	-2.15	-1.60	...	D69
	5	17.557	1.244	13.28	13.89	...	-2.23	-1.68	...	
	6	19.299	1.286	13.14	13.74	...	-2.37	-1.83	...	
	11	33.5	1.5	12.11	12.67	...	-3.40	-2.90	...	
	1	15.5647	1.1921	13.39	13.99	...	-2.12	-1.58	...	DC67
	5	17.557	1.244	13.24	13.86	...	-2.27	-1.71	...	
	6	19.299	1.286	13.06	13.70	...	-2.45	-1.87	...	
	11	33.475	1.525	12.24	12.90	...	-3.27	-2.67	...	
NGC 7492	4	17.9	1.3	14.21	15.81	...	-2.86	-1.26	...	B68

Note. — PR77=Pinto & Rosino (1977); CH89=Clement & Hazen (1989); BIC00=Borissova, Ivanov, & Catelan (2000); KK93=Kaluzny & Krzeminski (1993); DC67=Dickens & Carey (1967); SED02=Strader, Everitt, & Danford (2002); K97=Kaluzny et al. (1997); K68=Kwee (1968); WHB90=Wehlau, Hogg, & Butterworth (1990); Kopacki, Kołaczkowski, & Pigulski (2003); RR83=Russeva & Russev (1983); RIR82=Russeva, Ilieva, & Russev (1982); RR79=Russeva & Russev (1979); PM77=Pike & Meston (1977); D71=Demers (1971); CHY88=Clement, Hogg, & Yee (1988); Borissova, Catelan, & Valchev (2001); CHW85=Clement, Hogg, & Wells (1985); CH78=Clement & Hogg (1978); CHW80=Clement, Hogg, & Wells (1980); K01=Kopacki (2001); CIR84=Clement, Ip, & Robert (1984); WF94=Wehlau & Froelich (1994); DW71=Demers & Wehlau (1971); WB90=Wehlau & Butterworth (1990); WH84=Wehlau & Hogg (1984); WH78=Wehlau & Hogg (1978); LS00=Layden & Sarajedini (2000); L74=Lee (1974); WH85=Wehlau & Hogg (1985); B98=Butler et al. (1998); SS95=Silbermann & Smith (1995); H85=Harris (1985); D69=Demers (1969); B68=Barnes (1968)